Elsevier Editorial System(tm) for Experimental Eye Research

Manuscript Draft

Manuscript Number: EXER15-595R1

Title: Glio-vascular modifications caused by Aquaporin-4 deletion in the mouse retina

Article Type: Research article

Keywords: Aquaporin-4, Retina, Neuromyelitis Optica, Gliovascular biology, Blood-Retinal Barrier, Intraretinal Vasculature, Astrocytes, Muller cells

Corresponding Author: Prof. Grazia Paola Nicchia, PhD

Corresponding Author's Institution: University of Bari "Aldo Moro"

First Author: Grazia Paola Nicchia, PhD

Order of Authors: Grazia Paola Nicchia, PhD; Francesco Pisani, PhD; Laura Simone, PhD; Antonio Cibelli; Maria G Mola, PhD; Massimo Dal Monte, PhD; Antonio Frigeri, PhD; Paola Bagnoli, PhD; Maria Svelto

Abstract: Aquaporin-4 (AQP4) is the Central Nervous System water channel highly expressed at the perivascular glial domain. In the retina, two types of AQP4 expressing glial cells take part in the blood-retinal barrier (BRB), astrocytes and Müller cells. The aim of the present study is to investigate the effect of AQP4 deletion on the retinal vasculature by looking at typical pathological hallmark such as BRB dysfunction and gliotic condition.
AQP4 dependent BRB properties were evaluated by measuring the number of extravasations in WT and AQP4 KO retinas by Evans blue injection assay. AQP4 deletion did not affect the retinal vasculature, as assessed by Isolectin B4 staining, but caused BRB impairment to the deep plexus capillaries while the superficial and intermediate capillaries were not compromised. To investigate for gliotic responses caused by AQP4 deletion, Müller cells and astrocytes were analysed by immunofluorescence and western blot, using the Müller cell marker Glutamine Synthetase (GS) and the astrocyte marker GFAP. While GS expression was not altered in AQP4 KO retinas, a strong GFAP upregulation was found at the level of AQP4 KO astrocytes at the superficial plexus and not at Müller cells at the intermediate and deep plexi. These data, together with the upregulation of inflammatory markers (TNF-α, IL-6, IL-1β and ICAM-1) in AQP4 KO retinas indicated AQP4 deletion as responsible for a gliotic phenotype. Interestingly, no GFAP altered expression was found in AQP4 siRNA treated astrocyte primary cultures. All together these results indicate that AQP4 deletion is directly responsible for BRB dysfunction and gliotic condition in the mouse retina. The selective activation of glial cells at the primary plexus suggests that different regulatory elements control the reaction of astrocytes and Müller cells. Finally, GFAP upregulation is strictly linked to gliovascular crosstalk, as it is absent in astrocytes in culture. This study is useful to understand the role of AQP4 in the perivascular domain in the retina and its possible implications in the pathogenesis of retinal vascular diseases and of

Neuromyelitis Optica, a human disease characterized by anti-AQP4 auto-antibodies.

Cover Letter

Click here to download Cover Letter: UPLetter to the EditorEER16.docx

Dear Editor,

I would like to thank you for giving us the possibility to reconsider our revised paper to Experimental Eye Research (EER). In this revised version we have performed new experiments and we have responded to all the comments raised by the Reviewers.

We acknowledge the Reviewers for their time spent to provide central suggestion and comments. Their qualified contribution has improved the study significantly. We hope that this manuscript is now considered acceptable for publication in your journal.

Thank you for your consideration.

Yours sincerely,

Grazia Paola Nicchia

Highlights

1) AQP4 is important in maintaining the BRB integrity at the deep plexus;
2) AQP4 deletion causes an inflammatory response and a reactive phenotype restricted to astrocytes at the superficial plexus;
3) The astrocyte reaction is strictly linked to gliovascular crosstalk;
4) AQP4 deletion as the cause of GFAP upregulation in retinal astrocytes and not Muller cells indicates differential regulatory elements being involved in activation of astrocytes and Muller cells.

Point by point responses to the referee comments

Reviewer #1

1.In figure 1B it appears to me that the intermediate and deep layer seems to be the same. Could the authors provide another image for the deep layer vasculature?

The reviewer's comment is correct. We apologize for the mistake but some frames of the confocal analysis of the three layers were accidentally superimposed. Both reviewers having suggested the use of isolectin, as preferable to the use of CD31, new experiments have been performed in which isolectin has been used instead of CD31. A representative new figure, of better quality, has therefore been added as suggested.

2. Since the goal of this manuscript is to investigate the role of AQP4 in retinal vasculature it would be useful to show the retinal vasculature from the AQP4 KO. It is unclear if the vasculature in the deep layer is present or is abnormal and could explain the extravasation phenotype in the deep plexus. The authors can use isolectin to mark the vasculature.

We thank the reviewer for the very pertinent suggestion, which we agree to be crucial for such analysis. Isolectin staining was also suggested by Reviewer 2. The analysis has been performed and the new data added in Fig 1, accordingly.

3.For figure 5 can the authors provide a protein loading control?

The protein loading control has been added.

4.In the study by Pannicke et al., both inflammatory proteins as well as GFAP expression was assessed using RNA analysis. Though the RNA levels for the inflammatory proteins were higher (which is in agreement with the current manuscript), the GFAP levels were lower by 50%. It is difficult to reconcile their data with the current manuscript. Due to conflicting reports

on the phenotypes observed in these mice, it is important to discuss the various possibilities for the differences. This needs to be discussed since the differences could be due to some other factor that is not related to Aquaporin-4.

The point suggested by the reviewer has been added in the Discussion section (page 18).

Reviewer #2

In this manuscript "Glio-vascular modifications caused by Aquaporin-4 deletion in the moue retina" the authors Nicchia et al make a strong case for the regulation of BRB integrity in the retina deep vascular plexus by Aquaporin 4. The experiments are well performed and the data clearly presented. There are a few minor concerns

1. Please provide a comparative confocal image of retinal vasculature (stained with lectin) of aquaporin 4 null and wild-type mice. This will help determine if the vasculature is altered. It is difficult to determine this with the CD31 stain.

The image of the retinal vasculature stained with lectin has been added.

2. Please include a discussion about the recent report showing a synergistic relationship between TRPV4 and Aquaporin 4 channels in muller cells (J. Neuroscience 2015:35:13525-13537)

We agree that the relationship between TRPV4 and AQP4 is a very interesting point that we have added in the Discussion section as suggested (pages 19-20).

Graphical Abstract (for review)

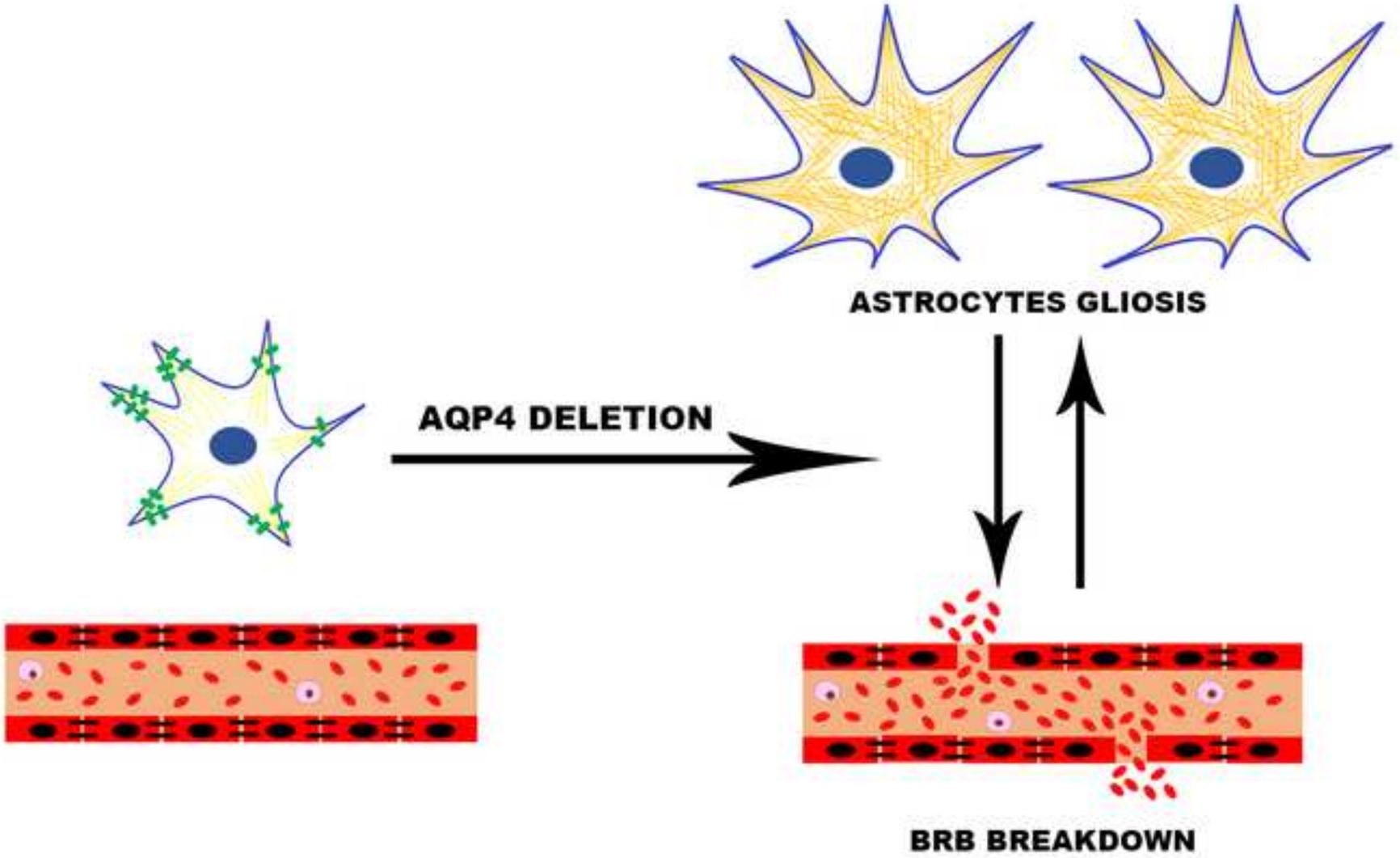

Glio-vascular modifications caused by Aquaporin-4 deletion in the mouse retina

Grazia Paola Nicchia[a, b, °,*], Francesco Pisani[a,°], Laura Simone[c], Antonio Cibelli[a], Maria Grazia Mola[a], Massimo Dal Monte[d], Antonio Frigeri[b,e], Paola Bagnoli[d], Maria Svelto[a,f,g]

[a]Department of Bioscience, Biotechnologies and Biopharmaceutics and Centre of Excellence in Comparative Genomics, University of Bari "Aldo Moro", 70126 Bari, Italy.
[b]Department of Neuroscience, Albert Einstein College of Medicine, New York, Bronx, NY, USA.
[c]IRCCS "Casa Sollievo della Sofferenza", Research Hospital, San Giovanni Rotondo, Italy.
[d]Department of Biology, University of Pisa, 56127, Pisa, Italy.
[e]School of Medicine: Basic Medical Sciences, Neuroscience and Sense Organs, University of Bari "Aldo Moro", 70126 Bari, Italy.
[f]Institute of Biomembranes and Bioenergetics, National Research Council, Via Amendola 165/A, 70126 Bari, Italy.
[g]National Institute of Biostructures and Biosystems (INBB), Viale Medaglie D'Oro 305, 00136 Rome, Italy.

°G.P. Nicchia and F. Pisani equally contributed to the study.

Corresponding author: *Grazia Paola Nicchia, Department of Bioscience, Biotechnologies and Biopharmaceutics and Centre of Excellence in Comparative Genomics, University of Bari "Aldo Moro", Bari, Italy. Tel: +39 080 5443335; Fax: +39 080 5443388; Email: graziapaola.nicchia@uniba.it*

Abbreviations: AQP4, Aquaporin-4; KO, knockout; WT, Wild-type; BRB, blood-retinal barrier; KD, knockdown; GFAP, Glial Fibrillary Acid Protein; qPCR, quantitative polymerase chain reaction; TNF-α, Tumor necrosis factor-α; IL-6, Interleukin-6; IL-1β, Interleukin 1β; ICAM-1, Intercellular adhesion molecule1; siRNA, small interfering RNA; CNS, Central Nervous System; BBB, blood-brain barrier; NFL, Nerve Fibre Layer; RGC, Retinal Ganglion cell; C-terminal, carboxyl-terminal; NMO, Neuromyelitis Optica; IgG, Immunoglobulin G; NFL, Nerve Fibre Layer; CD-31, Cluster of Differentiation; GAPDH, Glyceraldehyde 3-phosphate dehydrogenase; HRP, horseradish peroxidase; GS, Glutamine Synthetase; VEGF, vascular endothelial growth factor; IPL, Inner Plexiform Layer; INL, Inner Nuclear Layer; OPL, Outer Plexiform Layer; ONL, Outer Nuclear Layer.

ABSTRACT

Aquaporin-4 (AQP4) is the Central Nervous System water channel highly expressed at the perivascular glial domain. In the retina, two types of AQP4 expressing glial cells take part in the blood-retinal barrier (BRB), astrocytes and Müller cells. The aim of the present study is to investigate the effect of AQP4 deletion on the retinal vasculature by looking at typical pathological hallmark such as BRB dysfunction and gliotic condition.

AQP4 dependent BRB properties were evaluated by measuring the number of extravasations in WT and AQP4 KO retinas by Evans blue injection assay. AQP4 deletion did not affect the retinal vasculature, as assessed by Isolectin B_4 staining, but caused BRB impairment to the deep plexus capillaries while the superficial and intermediate capillaries were not compromised. To investigate for gliotic responses caused by AQP4 deletion, Müller cells and astrocytes were analysed by immunofluorescence and western blot, using the Müller cell marker Glutamine Synthetase (GS) and the astrocyte marker GFAP. While GS expression was not altered in AQP4 KO retinas, a strong GFAP upregulation was found at the level of AQP4 KO astrocytes at the superficial plexus and not at Müller cells at the intermediate and deep plexi. These data, together with the upregulation of inflammatory markers (TNF-α, IL-6, IL-1β and ICAM-1) in AQP4 KO retinas indicated AQP4 deletion as responsible for a gliotic phenotype. Interestingly, no GFAP altered expression was found in AQP4 siRNA treated astrocyte primary cultures. All together these results indicate that AQP4 deletion is directly responsible for BRB dysfunction and gliotic condition in the mouse retina. The selective activation of glial cells at the primary plexus suggests that different regulatory elements control the reaction of astrocytes and Müller cells. Finally, GFAP upregulation is strictly linked to gliovascular crosstalk, as it is absent in astrocytes in culture. This study is useful to understand the role of AQP4 in the perivascular domain in the retina and its possible implications in the pathogenesis of retinal vascular diseases and of Neuromyelitis Optica, a human disease characterized by anti-AQP4 auto-antibodies.

Keywords: Aquaporin-4, Retina, Neuromyelitis Optica, Gliovascular biology, Blood-Retinal Barrier, Intraretinal Vasculature, Astrocytes, Müller cells.

1. Introduction

Aquaporins are water channel proteins conferring a faster water flux to several cell plasma membranes in the presence of osmotic and hydrostatic gradients (Yang and Verkman, 1997). Aquaporin-4 (AQP4) is the Central Nervous System (CNS) water channel, which is highly concentrated at the perivascular glial end-feet and takes part in the blood-brain barrier functional unit (Amiry-Moghaddam et al., 2003; Frigeri et al., 1995; Nicchia et al., 2008).

In the retina, two types of AQP4 expressing glial cells take part in the blood-retinal barrier (BRB), astrocytes and Müller cells (Newman, 2001). Astrocyte end-feet control the barrier properties only at the level of the superficial plexus whereas Müller cell end-feet do so also at the level of intermediate and deep plexus. Müller cells generated inside the retina span into its entire thickness providing structural and functional support to neurons (Newman and Reichenbach, 1996). AQP4 would here control the osmotic imbalance caused by the high neuronal activity (Goodyear et al., 2009). The relationship between AQP4 and the Kir4.1 potassium channel in Müller cells in the control of potassium homeostasis (Bosco et al., 2005; Nagelhus et al., 1999) is considered the reason for the impaired light-neuronal signal transduction reported for AQP4 KO mouse retina (Li et al., 2002). Astrocytes are stellate, without orientation, enter the retina from the brain along the developing optic nerve (Stone and Dreher, 1987) and form a homogeneous plexus on the Nerve Fibre Layer (NFL) and Retinal Ganglion cell (RGC) layer. Astrocytes here play a key role in maintaining either the BRB properties or the survival of RGC, whose axons form the optic nerve. Though the role of AQP4 in maintaining water homeostasis in Müller cells has been extensively studied (Goodyear et al., 2009; Verkman et al., 2008), less attention has been paid to addressing its function under

normal conditions in the perivascular glial domain. Both Müller cells and astrocytes are enriched in intermediate filaments, however, Glial Fibrillary Acid Protein (GFAP) is the major component of the filaments in astrocytes (Dixon and Eng, 1981; Eng, 1985) but is found at very low levels in Müller cells (Bignami and Dahl, 1979). GFAP is thought to provide astrocytes with mechanical force as well as a particular shape, especially at the level of the terminal endfeet (Hyder et al., 2011). Several GFAP isoforms exist (Kamphuis et al., 2012), the canonical GFAP isoform is α, which is able to assemble in filaments based on a C-terminal motif that is instead absent in GFAPδ and κ, destabilizing the filaments (Blechingberg et al., 2007a; Hol and Pekny, 2015; Kamphuis et al., 2012).

BRB dysfunction and glial activation are key pathological features in a number of retinal vascular diseases, such as retinopathy of prematurity, diabetic retinopathy, and branch retinal vein occlusion, considered a primary cause of visual impairment and blindness (Coorey et al., 2012). Interestingly, altered AQP4 expression is also associated with some of these pathologies, such as branch retinal vein occlusion (Koferl et al., 2014) and diabetic retinopathy (Kumar et al., 2014; Qin et al., 2012). In diabetic rats, AQP4 knockdown (KD) leads to exacerbation of retinopathy with BRB dysfunction and inflammatory response (Cui et al., 2012). In Neuromyelitis Optica (NMO), a CNS autoimmune inflammatory “aquaporinopathy” affecting the optic nerve and spinal cord (Bergamaschi and Ghezzi, 2004; Jarius and Wildemann, 2010; Lennon et al., 2005; Lennon et al., 2004) and leading to paralysis and blindness, AQP4 is the molecular target of the autoantibody NMO IgG, the pathological hallmark of the disease. Interestingly, optic neuritis in NMO patients is characterized by retinal modifications at the vascular level and on the NFL (Camicione et al., 2010; Green and Cree, 2009; Merle et al., 2008), most likely caused by NMO IgG binding to AQP4 expressing cells in the retina and optic nerve.

Understanding the molecular basis of the role played by AQP4 at the level of retinal vasculature is fundamental for clarifying the pathogenesis of the diseases involving AQP4 dependent alterations in the retinal vasculature. Moreover, it will help in elucidating the role that glial cells play in the pathogenesis of such diseases, therefore supporting the developing of novel therapies. The aim of the present study is to investigate the effect of AQP4 deletion on the retinal vasculature by looking at typical pathological hallmark such as BRB dysfunction and gliotic condition.

2. Materials and Methods

2.1 Animals

5-10 month old AQP4 KO mice with a CD1 genetic background (Basco et al., 2013) and age matched controls were used. CD1 mice and Wistar rats were used for astrocyte primary cultures. Experiments were performed in accordance with the ARVO Statement for the Use of Animals in Ophthalmic and Vision Research and in compliance with the Italian law on animal care (Italian Health Department Approved Project n°100/2014-B). All experiments were designed to minimize the number of animals used and their suffering. The mice used here were bred in the approved facility at the University of Bari.

2.2 Antibodies

The following primary antibodies were used: goat polyclonal anti-AQP4 (Santa Cruz, CA, USA); goat polyclonal anti-CD31 (Santa Cruz, CA, USA); rabbit polyclonal anti-GFAP (Sigma-Aldrich, Milan, Italy); mouse monoclonal anti-GFAP (clone G-A-5, Millipore, Merck KGaA, Darmstadt, Germany); mouse monoclonal anti-GAPDH (MAB 374, Millipore, Merck KGaA, Darmstadt, Germany); mouse monoclonal anti-Glutamine Synthetase (MAB 302, Millipore, Merck); goat polyclonal anti-actin (Santa Cruz, CA, USA). The following secondary antibodies (all from Invitrogen, Milan, Italy) were used for immunofluorescence: donkey anti-goat Alexa Fluor488; donkey anti-mouse Alexa Fluor488; donkey anti-rabbit Alexa Fluor594; donkey anti-goat Alexa Fluor594; donkey anti-rabbit Alexa Fluor647. The following secondary antibodies (all from Santa Cruz, CA, USA) were used for Western blot:

goat anti-mouse IgG-horseradish peroxidase (HRP); goat anti-rabbit IgG-HRP; donkey anti-goat IgG-HRP.

2.3 Astrocyte primary cultures and RNA interference

Astrocytes were prepared from primary cell cultures of neocortical tissues as previously described (Nicchia et al., 2003). RNA interference experiments were performed as follows: astrocytes were transfected with 100 nM AQP4 siRNA smart pool or scrambled siRNA (Nicchia et al., 2003) by oligofectamine (Invitrogen, Milan, Italy), in a 24 multi-well format, according to the instruction manual, using high glucose GlutaMAX™ DMEM (Invitrogen, Milan, Italy), supplemented with 10% FBS (Invitrogen, Milan, Italy). After 10 days, cells were lysed with 100 µl of RIPA Buffer (see paragraph "western blot" for composition), and total protein content was measured using the Micro-BCA Protein Assay Kit (Thermo Scientific, Rockford, IL, USA). Five µl of proteins were analyzed by Western blot as later described.

2.4 Preparation of whole-mount retinas and retinal sections for immunofluorescence and Isolectin B_4 staining

Wild type (WT) and AQP4 KO mice were anesthetized by intraperitoneal injection of urethane (1.2 g/kg body weight). Retinas were explanted in ice cold PBS, washed several times and fixed with 4% paraformaldehyde (Sigma-Aldrich, Milan, Italy) for 60 min. For Isolectin staining, retinas were permeabilized overnight with 0.5% Triton X-100 in PBS, washed several times in PBS and incubated overnight with 10 µg/ml of FITC-conjugated Isolectin B_4 (IB4) from Bandeiraea simplicifolia (Griffonia simplicifolia). After washings in PBS, retinas were finally mounted in PBS-glycerol

(1:1) pH 8.0, containing 1% n-propyl gallate. For immunofluorescence, after fixation retinas were washed in PBS, permeabilized with 0.5% Triton X-100 in PBS for 30 min and saturated for 30 min with 1% BSA, 0.5% Triton X-100 in PBS. All these steps were performed at RT. Retinas were incubated with primary antibodies for 48h at 4°C in 1% BSA in PBS, washed three times with 1% BSA, 0.5% Triton X-100 in PBS for 20 min each and then incubated with secondary antibodies (1:1000 dilution) and isolectin B_4 (10 µg/ml) for 24 h in the same solution at 4°C. The day after, the retinas were washed three times in PBS, and finally mounted in PBS-glycerol (1:1) pH 8.0, containing 1% n-propyl gallate. For section preparation, enucleated eyes were fixed in 4% PFA solution for 2-3 hours at 4°C. After removal of cornea, iris and lens, whole posterior eyecups were immersed in 30% sucrose solution in PBS overnight; then, eyescups were embedded in OCT compound (Leica Biosystem, Nussloch, Germany) and immediately frozen at -80°C. Sections of 10-µm thickness were cut on a cryostat at -20°C. After blocking, sections were incubated with primary antibodies overnight at 4°C in blocking solution (0.1% Gelatin in PBS), washed for 30 min and then incubated with secondary antibodies for 1 h. Finally, the sections were washed for 30 min in PBS and mounted in PBS-glycerol (1:1) pH 8.0, containing 1% n-propyl gallate.

2.5 Confocal microscopy analysis

Confocal images were obtained with an automated inverted Leica TCS SP8 confocal microscope using a 16x and 63x HC PL Apo oil CS2 objective. 3D-images and projections from the z-stack were constructed and processed using Leica Application Suite X software.

2.6 Protein extraction from retinas, Western blot and densitometric analysis

Eyes were harvested from WT and AQP4 KO mice, and immediately dissected in ice cold PBS. Excessive liquid was removed, retinas snap-frozen in liquid nitrogen and stored at -80°C. Proteins were extracted from stored explanted retinas in 7-10 volumes of RIPA buffer (10 mM Tris-HCl, pH 7.4; 140 mM NaCl; 1% Triton X-100; 1% Na deoxycholate; 0.1% SDS; 1 mM Na_3VO_4; 1 mM NaF and 1 mM EDTA) added with a cocktail of protease inhibitors (Roche, Milan, Italy). The lysis was performed on ice for 1h and the samples were then centrifuged at 22,000xg for 1h. The protein content of the supernatant was measured with a bicinchoninic acid (BCA) Protein Assay Kit (Pierce, Rockford, IL, USA). 30 µg of protein samples was loaded in NuPAGE 4-12% Bis-Tris Gel (Invitrogen, Milan, Italy) and transferred to polyvinylidene difluoride membranes (Millipore, Milan, Italy), as described previously (Pisani et al., 2014). Membranes with blotted proteins were incubated with primary antibodies, washed, and incubated with peroxidase-conjugated secondary antibodies (Nicchia et al., 2003). Reactive proteins were revealed using an enhanced chemiluminescent detection system (ECL Plus, Thermo scientific, Rockford, IL, USA) and visualized on a Versadoc imaging system (BioRad, Milan, Italy). Densitometry analysis was performed using ImageJ Software (National Institute of Mental Health, Bethesda, Maryland, USA) and analyzed by GraphPad Prism 5 (GraphPad, San Diego, USA).

2.7 qPCR

RNA extraction was carried out using Trizol Reagent (Invitrogen, Milan, Italy) according to the instruction manual. Total RNA was quantified by Nanodrop

(Thermo scientific, Waltham, MA, USA). 3 µg of total RNA were retrotranscribed by SuperScript III Reverse Transcriptase (Invitrogen, Milan, Italy). GFAP isoform expression was measured by the GAPDH normalized ΔΔCt quantification method using previously published primers (Kamphuis et al., 2012). Sybr Green (Invitrogen, Milan, Italy) and StepOne (Applied Biosystems) were used. Instead, the expression of Tumor necrosis factor-α (TNF-α), Intercellular adhesion molecule1 (ICAM-1), Interleukin (IL)-1β and IL-6 was measured by the Rpl13a normalized ΔΔCt quantification method using previously published primers (Dal Monte et al., 2015).

2.8 Evans Blue assay

Mice retinal blood vessel permeability was tested by Evans Blue assay as follows: 300µl of Evans Blue (30 mg/ml) in PBS was intraperitoneally injected. After 20 min, retinas were explanted and extravasation evaluated by epifluorescence analysis at an excitation wavelength of 594nm with a Leica DM RXA microscope using a 16x oil PL FL FLUOTAR objective. Five digital images from each quadrant for each retina were recorded and processed using Las AF software and the number of extravasations manually counted.

2.9 Statistical analysis

Mean ± standard error is reported in the results. Statistical analysis was performed using GraphPad Prism 5 (GraphPad, San Diego, USA) by ANOVA or t-test for unpaired data. A p value < 0.05 was considered statistically significant.

3. Results

3.1 Impaired BRB functionality at the AQP4 KO deep plexus

The relationship between the intraretinal vasculature and macroglial cells is shown in Fig. 1A. The drawing shows that the superficial plexus is ensheathed by glial cell processes arising mainly from astrocytes while the intermediate and deep plexi are ensheathed by glial processes arising from Müller cells. To analyze AQP4 expression at the gliovascular interface, confocal microscopy experiments were performed on the whole retina, using the astrocyte marker GFAP and IB4 to stain the retinal vasculature (Fig. 1B, C). At the superficial plexus, GFAP expression at the level of astrocytes was very strong, as expected. AQP4 staining was here concentrated at the perivascular level but there was also AQP4 signal coming from Muller cells processes uniformly distributed within the layer under analysis. GFAP staining was found to be very low at the intermediate and the deep plexi, the glial part here being represented by Müller cells. The capillaries here appeared to be very well depicted by AQP4 staining, indicating very highly concentrated AQP4 expression in the perivascular glial processes (Fig. 1B). Fig. 1C shows a z-stack distribution of GFAP, AQP4 and IB4 expression depending on the depth of the whole retina analysed by confocal microscopy. This analysis highlights that GFAP signal is concentrated at the superficial plexus while AQP4 and IB4 overlap at the three plexi, indicating that intraretinal vasculature is completely ensheathed by glial processes with highly enriched AQP4 water channels. AQP4 concentrated fluorescence at the deep plexus corresponds to its high expression at Muller cells.

To investigate whether AQP4 KO mice are characterized by intraretinal vascular abnormalities, confocal microscopy analysis was performed on WT and AQP4 KO

retinas stained with IB4. Separate images, acquired for each plexus (Fig. 1D) revealed no differences, indicating that AQP4 deletion does not cause intaretinal structural alteration at the vascular level.

AQP4 dependent BRB properties were then evaluated by measuring the number of extravasations in WT and AQP4 KO retinas by Evans blue injection assay. Treated retinas were isolated and analysed by epifluorescence (Fig. 2A) and confocal microscopy (Fig. 2B-C). Epifluorescence analysis, performed to quantify the number of extravasations, allowed us to associate a statistically significant higher number of extravasations to AQP4 KO retinas (Fig. 2A). By confocal microscopy, the extravasations were localized at the deep plexus capillaries while the superficial and intermediate plexus were not compromised (Fig. 2B,C). These data point to AQP4 absence being responsible for functional alterations at the BRB level, which are evident at the deep plexus, where AQP4 is highly concentrated.

3.2 Muller cells, identified by Glutamine Synthetase expression, do not show alterations in the retina of AQP4 KO mice

In order to investigated gliotic responses caused by AQP4 deletion in the retina, Müller cells and astrocytes were analysed by immunofluorescence on retinal sections and western blot, using the Muller cell marker Glutamine Synthetase (Fig. 3) and the astrocyte marker GFAP (Fig. 4). We observed that pattern and intensity of GS immunoreactivity was not altered in the absence of AQP4 (Fig. 3A), in line with WB results showing comparable GS expression level between WT and AQP4 KO retinas (Fig. 3B,C). These results indicate the absence of a major impact of AQP4 deletion on retinal Muller cells.

3.3 Reactive phenotype of AQP4 KO superficial plexus assessed by strong GFAP upregulation

The hypothesis of a gliotic phenotype to explain structural alterations at AQP4 KO gliovascular interface was also investigated by the analysis of GFAP expression by immunolocalization on cryosectioned retinas and whole-mount retina, by Western blot and qPCR (Fig. 4, Fig.5). GFAP immunolocalization on retinal sections (Fig. 4A) showed a grossly comparable GFAP distribution between WT and AQP4 KO retinas although the signal appeared stronger in AQP4 KO ones. For Western blot, the analysis was carried out to discriminate between the relative expression of the most characterized GFAP isoforms, GFAPα, δ, and κ. To this end, a monoclonal antibody (clone G-A-5), able to selectively recognize these isoforms, was used (Fig. 4B). Western blot results revealed that all the GFAP isoforms were significantly upregulated in AQP4 KO vs WT (Fig. 4 C,D). Finally, the quantitative analysis of gene expression demonstrated mRNA level of GFAPα and GFAPδ increase of 2 fold in the AQP4 KO mice compared with WT mice, while mRNA expression level of GFAPκ showed a 10 fold increase (Fig. 4 E). The results obtained for GFAP at the mRNA level were in line with those obtained for GFAP protein with a particular upregulation of GFAPκ.

GFAP upregulation in AQP4 KO was then more deeply investigated by confocal microscopy on whole mount retinas (Fig. 5). Immunofluorescence results revealed a strong GFAP overexpression only at the level of the AQP4 KO superficial plexus. No GFAP upregulation was detected at the intermediate or deep plexi.

Altogether, these data indicate that a gliotic phenotype, with a GFAP upregulation, is selectively acquired by AQP4 KO astrocytes at the superficial plexus and not by Müller cells at the intermediate and deep plexi.

3.4 AQP4 KD does not alter GFAP expression in astrocyte primary cultures

The direct cause-effect relationship between AQP4 deletion and the altered expression of GFAP isoforms observed in AQP4 KO retinas was then investigated in a cell culture system outside the gliovascular environment (Fig. 6). We decided to take advantage of primary astrocyte cultures characterized by AQP4 reduced expression, such as AQP4 KD astrocytes obtained by RNA interference (Nicchia et al., 2005). By Western blot, we analysed GFAP expression in rat and mouse primary culture of astrocytes treated with specific AQP4 siRNA for 10 days and no difference was found, GFAPα being the only isoform expressed. These data demonstrate that loss of AQP4 expression is not a direct cause of GFAP alterations outside the gliovascular environment.

3.5 Inflammatory pattern in AQP4 KO retinas

The inflammatory state of AQP KO retinas was analysed (Fig. 7) by measuring the level of proinflammatory cytokines such as IL-1β, IL-6, TNF-α and the intercellular adhesion molecule (ICAM-1), this last being upregulated following exposure to proinflammatory stimuli such as TNF-α and IL-1β (Eddleston and Mucke, 1993). Quantitative analysis of gene expression by qPCR demonstrated that mRNA level of IL-1β and TNF-α increased around 3 folds in AQP4 KO compared to WT while

mRNA expression level of IL-6 increased 7 folds and of ICAM-1 2 folds. These data indicate that AQP4 absence in the retina is responsible for an inflammatory status.

4. Discussion

The breakdown of BRB is a common feature of several retinal vascular diseases and it is often associated with an inflammatory response (Coorey et al., 2012). We here show that AQP4 deletion causes BRB extravasations exclusively localized at the deep plexus of the retina where normally AQP4 is very highly concentrated. A possible explanation for the difference in BRB extravasation is that the deep plexus smaller calibre vessels, being more fragile, become more susceptible to BRB dysfunction in the absence of AQP4. We cannot exclude however, that AQP4 deletion may cause a polarized release of paracrine factors responsible for the increase in BRB permeability. For instance, AQP4 KD in cultured rat Müller cells enhances the release of vascular endothelial growth factor (VEGF) (Shelton et al., 2009), and it has been demonstrated that Müller cell-derived VEGF plays an essential and causative role in vascular lesions and vascular leakage in diseased retinas (Wang et al., 2010). Interestingly, pathological conditions, such as diabetic retinopathy (Kumar et al., 2014; Qin et al., 2012), as well as transient retinal ischemia (Hirrlinger et al., 2010; Koferl et al., 2014) and retinal injury (Dibas et al., 2008; Iandiev et al., 2008) are characterized by BRB dysfunctions and by an altered expression of both AQP4 and GFAP (Cui et al., 2012). The hypothesis of a gliotic condition, as a consequence of AQP4 deletion, was therefore investigated. GFAP, normally used to identify astrocytes in the CNS, is also a very well known marker of active gliosis, being upregulated after traumatic injury and neuronal degeneration. In the retina, under normal conditions, it is expressed by astrocytes, and at a very low level by Müller cells. However, it is has been reported that, in response to retinal injury or photoreceptor degeneration, GFAP expression is activated in Müller cells and becomes a marker of retinal gliosis (Ekstrom et al., 1988). Interestingly, there is

a study by Verderber et al., (Verderber et al., 1995) reporting that regulatory elements, which determine GFAP induction in Müller cells, are different from those involved in GFAP expression in astrocytes. We here show that AQP4 deletion causes a strong upregulation of GFAP at the perivascular astrocytes of the superficial layer and not at perivascular Müller cells at the intermediate and deep plexi. This data, here supported by the altered inflammatory pattern found in AQP4 KO retinas, strongly indicates a gliotic condition primarily affecting the GCL.

The function of reactive gliosis and, in particular, whether it is pathological or beneficial is still controversial (Verkhratsky et al., 2012). We here show BRB impairment at the deep plexus, which is not interested by a gliotic condition and, viceversa, BRB integrity at the superficial plexus where a gliotic condition is identified by GFAP upregulation. This scenario could be considered an example of gliosis as a “beneficial reaction” occurring at the superficial plexus with the aim to protect the integrity of the BRB. In line with this view, we can further speculate that the absence of glial activation at the deep plexus is one of the causes for the impaired BRB observed.

AQP4 KO retinas have been previously analysed by Li et al. (2002) and no difference in ultrastructure was reported but a mild impaired retinal function was found (Li et al., 2002). However, a more recent study by Pannicke et al (Pannicke et al., 2010), performed on the same AQP4 KO mice used by Li et al (2002), shows that deletion of AQP4 is associated with a distinct inflammatory response of the retina, which is in agreement with our results. The same study, however, reported a significant reduction in GFAP mRNA in AQP4 KO retinas while GFAP protein expression, evaluated by immunolocalization, was not altered. Although, protein levels cannot be accurately determined by immunofluorescence and no WB were performed in the study by Li, the unaltered GFAP protein expression could be

explained because the analysis by immunofluorescence was carried out on cross sections showing the retinal layers, not as informative for astrocyte details as by longitudinal analysis showing each plexus. It is more difficult to explain the discrepancy between the reduced GFAP mRNA expression with the significant increase here shown instead. Although, in general, reduced mRNA expression not followed by a parallel decrease in the relative protein expression does not have a physiological significance, the only explanations for such a discrepancy are either the mouse model used or the age of the animals. Differences in the phenotype of these mice (Owler et al., 2010), unrelated with AQP4, could be at the base of the discrepancy on GFAP mRNA levels in AQP4 KO mice. Alternatively, this difference could be ascribable to the use of younger mice (3-4 months old) by Pannicke. Future study will be focused on age dependent alteration of GFAP mRNA and protein in AQP4 KO mice. However, we believe it is important to highlight that, independently of the up or down regulation of GFAP mRNA, and despite phenotype differences, an altered inflammation pattern is observed in both mouse models.

Considering that reactive astrocytes in the retina lead to RGC death and contribute to visual impairment (Ganesh and Chintala, 2011), we can here propose that the impaired retinal function found in AQP4 KO mice (Li et al., 2002), so far attributed only to Müller cell alteration, can also be ascribed to the presence of an inflammatory response of the superficial plexus, causing neuronal damage and optic nerve impairment. Moreover, AQP4 deletion as the cause of GFAP upregulation in retinal astrocytes and not in Müller cells is a further support for differential regulatory elements being involved in the activation of the two types of macroglial cells (Verderber et al., 1995).

While GFAPα is the canonical isoform characteristic of healthy glial cells (Kamphuis et al., 2012; Moeton et al., 2014), isoforms δ and κ are differentially expressed in

pathological conditions. In particular, GFAPk is increased in multiform glioblastoma (Blechingberg et al., 2007a; Blechingberg et al., 2007b). Our data show a particular upregulation of GFAPk mRNA in AQP4 KO retina, in line with the observed pathological signs.

AQP4 deletion as the direct cause of a GFAP altered expression has been also investigated here using primary astrocyte cultures lacking AQP4, in particular, AQP4 siRNA treated astrocytes (Nicchia et al., 2003). We show that AQP4 KD in culture is not sufficient to produce any alteration in GFAP isoform expression even if the KD is prolonged by up to ten days. Therefore, we can conclude that AQP4 absence in cultured astrocytes does not cause a gliotic phenotype, which seems strictly dependent on a glio-vascular crosstalk. This result may find an explanation on the basis of the culture conditions of astrocytes outside their own *in vivo* environment in which AQP4 expression is maintained but its typical polarized expression is lost, the water flux being strictly linked to the transport of molecules and ions normally occurring at the perivascular glial processes (Nicchia et al., 2000). On the basis of the evidence from studies on astrocytes in cultures, we can assume that the inflammatory condition, indicated by GFAP upregulation and by the upregulation of the inflammatory markers, is strictly linked to a gliovascular expression of AQP4.

During pathological situations in the CNS, such as cerebral ischemia, a rapid intracellular calcium increase triggers reactive gliosis (Verkhratsky et al., 2009). Interestingly, synergic cooperation between AQP4 and the polymodal transient receptor potential vanilloid 4 (TRPV4) channel has been proposed, in controlling calcium homeostasis in astrocytes (Benfenati et al., 2011; Mola et al., 2016) and Müller cells (Jo et al., 2015). In particular, the mechanisms proposed by Jo et al. and Mola et al. are very similar in highlighting a functional, rather than physical,

interaction, strictly linked to the effect of AQP-dependent fast water flux on the level of plasma membrane stretch and therefore on TRPV4 activation. We can speculate that a physiological diversity between astrocytes and Müller cells in sensing and modulating calcium homeostasis and in controlling the downstream mechanism involved in calcium dependent gliosis, can be at the base of their different reaction to AQP4 deletion.

5. Conclusion

In conclusion, we here show that AQP4 deletion causes BRB dysfunction at the deep plexus, an inflammatory status and a reactive phenotype, most likely beneficial, restricted to the superficial plexus with GFAP upregulation. The possibilities are: 1) The altered water homeostasis caused by AQP4 deletion is the direct cause of both BRB impairment and astrocyte activation. If this is the case, the AQP4 dependent reactive condition would be strictly linked to gliovascular crosstalk, which is absent when astrocytes are placed in culture; 2) AQP4 deletion causes BRB dysfunction in turn causing an astrocyte reaction. In this case, the GFAP upregulation found would be the consequence of extravasation of fluid and inflammatory factors, causing the inflammatory response. The reason why, however, those factors would act only on astrocytes and not on Müller cells would be unclear; 3) AQP4 deletion is a direct cause of astrocyte activation with an inflammatory response in turn responsible for BRB impairment.

We believe this study adds knowledge on the modification occurring in the absence of AQP4 useful in understanding its role in retinal glial cells under normal conditions and helps in elucidating the molecular basis leading to BRB breakdown and glial activation in the retina. Moreover, it provides important pieces of information on the

role that AQP4 may play in the pathogenesis of retinal vascular diseases, such as such as branch retinal vein occlusion and diabetic retinopathy and NMO. In particular, in future studies, it will be important to address whether BRB impairment and/or an inflammatory response are involved in optic neuritis caused by NMO IgG binding to AQP4 expressing glial cells in NMO patients.

Acknowledgments

The authors would like to thank Richard Lusardi for his assistance in revising the English of the article, Gaetano De Vito for his excellent technical assistance, and Francesca Sanarica for her support in retinal explantation and technical assistance.

This study was financed by the Italian Ministry of University and Research (Project Firb “Futuro in Ricerca” RBFR12SJA8 to Grazia Paola Nicchia) and by the Italian Ministry of Health 2014-2017 (Project Biomedical RF-2011-02351158 to Paola Bagnoli).

References

Amiry-Moghaddam, M., Otsuka, T., Hurn, P.D., Traystman, R.J., Haug, F.M., Froehner, S.C., Adams, M.E., Neely, J.D., Agre, P., Ottersen, O.P., Bhardwaj, A., 2003. An alpha-syntrophin-dependent pool of AQP4 in astroglial end-feet confers bidirectional water flow between blood and brain. Proc Natl Acad Sci U S A 100, 2106-2111.

Basco, D., Blaauw, B., Pisani, F., Sparaneo, A., Nicchia, G.P., Mola, M.G., Reggiani, C., Svelto, M., Frigeri, A., 2013. AQP4-Dependent Water Transport Plays a Functional Role in Exercise-Induced Skeletal Muscle Adaptations. PLoS One 8, e58712.

Benfenati, V., Caprini, M., Dovizio, M., Mylonakou, M.N., Ferroni, S., Ottersen, O.P., Amiry-Moghaddam, M., 2011. An aquaporin-4/transient receptor potential vanilloid 4 (AQP4/TRPV4) complex is essential for cell-volume control in astrocytes. Proc Natl Acad Sci U S A 108, 2563-2568.

Bergamaschi, R., Ghezzi, A., 2004. Devic's neuromyelitis optica: clinical features and prognostic factors. Neurol Sci 25 Suppl 4, S364-367.

Bignami, A., Dahl, D., 1979. The radial glia of Muller in the rat retina and their response to injury. An immunofluorescence study with antibodies to the glial fibrillary acidic (GFA) protein. Experimental eye research 28, 63-69.

Blechingberg, J., Holm, I.E., Nielsen, K.B., Jensen, T.H., Jorgensen, A.L., Nielsen, A.L., 2007a. Identification and characterization of GFAPkappa, a novel glial fibrillary acidic protein isoform. Glia 55, 497-507.

Blechingberg, J., Lykke-Andersen, S., Jensen, T.H., Jorgensen, A.L., Nielsen, A.L., 2007b. Regulatory mechanisms for 3'-end alternative splicing and polyadenylation of the Glial Fibrillary Acidic Protein, GFAP, transcript. Nucleic Acids Res 35, 7636-7650.

Bosco, A., Cusato, K., Nicchia, G.P., Frigeri, A., Spray, D.C., 2005. A developmental switch in the expression of aquaporin-4 and Kir4.1 from horizontal to Muller cells in mouse retina. Invest Ophthalmol Vis Sci 46, 3869-3875.

Camicione, P., Fodor, E., Pannarello, S., Barabino, S., 2010. Retinal peripapillary nerve fiber layer thickness in a 13-year-old boy with neuromyelitis optica. European journal of ophthalmology 20, 485-488.

Coorey, N.J., Shen, W., Chung, S.H., Zhu, L., Gillies, M.C., 2012. The role of glia in retinal vascular disease. Clinical & experimental optometry : journal of the Australian Optometrical Association 95, 266-281.

Cui, B., Sun, J.H., Xiang, F.F., Liu, L., Li, W.J., 2012. Aquaporin 4 knockdown exacerbates streptozotocin-induced diabetic retinopathy through aggravating inflammatory response. Exp Eye Res 98, 37-43.

Dal Monte, M., Rezzola, S., Cammalleri, M., Belleri, M., Locri, F., Morbidelli, L., Corsini, M., Paganini, G., Semeraro, F., Cancarini, A., Rusciano, D., Presta, M., Bagnoli, P., 2015. Antiangiogenic Effectiveness of the Urokinase Receptor-Derived Peptide UPARANT in a Model of Oxygen-Induced Retinopathy. Invest Ophthalmol Vis Sci 56, 2392-2407.

Dibas, A., Yang, M.H., He, S., Bobich, J., Yorio, T., 2008. Changes in ocular aquaporin-4 (AQP4) expression following retinal injury. Mol Vis 14, 1770-1783.

Dixon, R.G., Eng, L.F., 1981. Glial fibrillary acidic protein in the optic nerve of the developing albino rat: an immunoperoxidase study of paraffin-embedded tissue. The Journal of comparative neurology 201, 15-24.

Eddleston, M., Mucke, L., 1993. Molecular profile of reactive astrocytes--implications for their role in neurologic disease. Neuroscience 54, 15-36.

Ekstrom, P., Sanyal, S., Narfstrom, K., Chader, G.J., van Veen, T., 1988. Accumulation of glial fibrillary acidic protein in Muller radial glia during retinal degeneration. Investigative ophthalmology & visual science 29, 1363-1371.

Eng, L.F., 1985. Glial fibrillary acidic protein (GFAP): the major protein of glial intermediate filaments in differentiated astrocytes. Journal of neuroimmunology 8, 203-214.

Frigeri, A., Gropper, M.A., Umenishi, F., Kawashima, M., Brown, D., Verkman AS., 1995. Localization of MIWC and GLIP water channel homologs in neuromuscular, epithelial and glandular tissues. J Cell Sci 108, 2993-3002.

Ganesh, B.S., Chintala, S.K., 2011. Inhibition of reactive gliosis attenuates excitotoxicity-mediated death of retinal ganglion cells. PLoS One 6, e18305.

Goodyear, M.J., Crewther, S.G., Junghans, B.M., 2009. A role for aquaporin-4 in fluid regulation in the inner retina. Vis Neurosci 26, 159-165.

Green, A.J., Cree, B.A., 2009. Distinctive retinal nerve fibre layer and vascular changes in neuromyelitis optica following optic neuritis. Journal of neurology, neurosurgery, and psychiatry 80, 1002-1005.

Hirrlinger, P.G., Ulbricht, E., Iandiev, I., Reichenbach, A., Pannicke, T., 2010. Alterations in protein expression and membrane properties during Muller cell gliosis in a murine model of transient retinal ischemia. Neurosci Lett 472, 73-78.

Hol, E.M., Pekny, M., 2015. Glial fibrillary acidic protein (GFAP) and the astrocyte intermediate filament system in diseases of the central nervous system. Curr Opin Cell Biol 32, 121-130.

Hyder, C.L., Isoniemi, K.O., Torvaldson, E.S., Eriksson, J.E., 2011. Insights into intermediate filament regulation from development to ageing. J Cell Sci 124, 1363-1372.

Iandiev, I., Pannicke, T., Hollborn, M., Wiedemann, P., Reichenbach, A., Grimm, C., Reme, C.E., Bringmann, A., 2008. Localization of glial aquaporin-4 and Kir4.1 in the light-injured murine retina. Neurosci Lett 434, 317-321.

Jarius, S., Wildemann, B., 2010. AQP4 antibodies in neuromyelitis optica: diagnostic and pathogenetic relevance. Nature reviews. Neurology 6, 383-392.

Jo, A.O., Ryskamp, D.A., Phuong, T.T., Verkman, A.S., Yarishkin, O., MacAulay, N., Križaj, D., 2015. TRPV4 and AQP4 Channels Synergistically Regulate Cell Volume and Calcium Homeostasis in Retinal Müller Glia. J Neurosci 35, 13525-13537.

Kamphuis, W., Mamber, C., Moeton, M., Kooijman, L., Sluijs, J.A., Jansen, A.H., Verveer, M., de Groot, L.R., Smith, V.D., Rangarajan, S., Rodriguez, J.J., Orre, M., Hol, E.M., 2012. GFAP isoforms in adult mouse brain with a focus on neurogenic astrocytes and reactive astrogliosis in mouse models of Alzheimer disease. PLoS One 7, e42823.

Koferl, P., Hollborn, M., Rehak, J., Iandiev, I., Dukic-Stefanovic, S., Wiedemann, P., Kohen, L., Bringmann, A., Rehak, M., 2014. Effects of arteriolar constriction on retinal gene expression and Muller cell responses in a rat model of branch retinal vein occlusion. Graefes Arch Clin Exp Ophthalmol 252, 257-265.

Kumar, B., Gupta, S.K., Nag, T.C., Srivastava, S., Saxena, R., Jha, K.A., Srinivasan, B.P., 2014. Retinal neuroprotective effects of quercetin in streptozotocin-induced diabetic rats. Exp Eye Res 125, 193-202.

Lennon, V.A., Kryzer, T.J., Pittock, S.J., Verkman, A.S., Hinson, S.R., 2005. IgG marker of optic-spinal multiple sclerosis binds to the aquaporin-4 water channel. J Exp Med 202, 473-477.

Lennon, V.A., Wingerchuk, D.M., Kryzer, T.J., Pittock, S.J., Lucchinetti, C.F., Fujihara, K., Nakashima, I., Weinshenker, B.G., 2004. A serum autoantibody marker of neuromyelitis optica: distinction from multiple sclerosis. Lancet 364, 2106-2112.

Li, J., Patil, R.V., Verkman, A.S., 2002. Mildly abnormal retinal function in transgenic mice without Muller cell aquaporin-4 water channels. Invest Ophthalmol Vis Sci 43, 573-579.

Merle, H., Olindo, S., Donnio, A., Richer, R., Smadja, D., Cabre, P., 2008. Retinal peripapillary nerve fiber layer thickness in neuromyelitis optica. Investigative ophthalmology & visual science 49, 4412-4417.

Moeton, M., Kanski, R., Stassen, O.M., Sluijs, J.A., Geerts, D., van Tijn, P., Wiche, G., van Strien, M.E., Hol, E.M., 2014. Silencing GFAP isoforms in astrocytoma cells disturbs laminin-dependent motility and cell adhesion. FASEB J 28, 2942-2954.

Mola, M.G., Sparaneo, A., Gargano, C.D., Spray, D.C., Svelto, M., Frigeri, A., Scemes, E., Nicchia, G.P., 2016. The speed of swelling kinetics modulates cell volume regulation and calcium signaling in astrocytes: A different point of view on the role of aquaporins. Glia 64, 139-154.

Nagelhus, E.A., Horio, Y., Inanobe, A., Fujita, A., Haug, F.M., Nielsen, S., Kurachi, Y., Ottersen, O.P., 1999. Immunogold evidence suggests that coupling of K+ siphoning and water transport in rat retinal Muller cells is mediated by a coenrichment of Kir4.1 and AQP4 in specific membrane domains. Glia 26, 47-54.

Newman, E., Reichenbach, A., 1996. The Muller cell: a functional element of the retina. Trends in neurosciences 19, 307-312.

Newman, E.A., 2001. Propagation of intercellular calcium waves in retinal astrocytes and Muller cells. The Journal of neuroscience : the official journal of the Society for Neuroscience 21, 2215-2223.

Nicchia, G.P., Frigeri, A., Liuzzi, G.M., Santacroce, M.P., Nico, B., Procino, G., Quondamatteo, F., Herken, R., Roncali, L., Svelto, M., 2000. Aquaporin-4-containing astrocytes sustain a temperature- and mercury-insensitive swelling in vitro. Glia 31, 29-38.

Nicchia, G.P., Frigeri, A., Liuzzi, G.M., Svelto, M., 2003. Inhibition of aquaporin-4 expression in astrocytes by RNAi determines alteration in cell morphology, growth, and water transport and induces changes in ischemia-related genes. FASEB journal : official publication of the Federation of American Societies for Experimental Biology 17, 1508-1510.

Nicchia, G.P., Rossi, A., Nudel, U., Svelto, M., Frigeri, A., 2008. Dystrophin-dependent and -independent AQP4 pools are expressed in the mouse brain. Glia 56, 869-876.

Nicchia, G.P., Srinivas, M., Li, W., Brosnan, C.F., Frigeri, A., Spray, D.C., 2005. New possible roles for aquaporin-4 in astrocytes: cell cytoskeleton and functional relationship with connexin43. Faseb J 19, 1674-1676.

Owler, B.K., Pitham, T., Wang, D., 2010. Aquaporins: relevance to cerebrospinal fluid physiology and therapeutic potential in hydrocephalus. Cerebrospinal Fluid Res 7:15.

Pannicke, T., Wurm, A., Iandiev, I., Hollborn, M., Linnertz, R., Binder, D.K., Kohen, L., Wiedemann, P., Steinhauser, C., Reichenbach, A., Bringmann, A., 2010. Deletion of aquaporin-4 renders retinal glial cells more susceptible to osmotic stress. J Neurosci Res 88, 2877-2888.

Pisani, F., Mola, M.G., Simone, L., Rosito, S., Alberga, D., Mangiatordi, G.F., Lattanzi, G., Nicolotti, O., Frigeri, A., Svelto, M., Nicchia, G.P., 2014. Identification of a point mutation impairing the binding between aquaporin-4 and neuromyelitis optica autoantibodies. J Biol Chem 289, 30578-30589.

Qin, Y., Ren, H., Hoffman, M.R., Fan, J., Zhang, M., Xu, G., 2012. Aquaporin changes during diabetic retinopathy in rats are accelerated by systemic hypertension and are linked to the renin-angiotensin system. Invest Ophthalmol Vis Sci 53, 3047-3053.

Shelton, M.D., Distler, A.M., Kern, T.S., Mieyal, J.J., 2009. Glutaredoxin regulates autocrine and paracrine proinflammatory responses in retinal glial (muller) cells. The Journal of biological chemistry 284, 4760-4766.

Stone, J., Dreher, Z., 1987. Relationship between astrocytes, ganglion cells and vasculature of the retina. The Journal of comparative neurology 255, 35-49.

Verderber, L., Johnson, W., Mucke, L., Sarthy, V., 1995. Differential regulation of a glial fibrillary acidic protein-LacZ transgene in retinal astrocytes and Muller cells. Investigative ophthalmology & visual science 36, 1137-1143.

Verkhratsky, A., Anderova, M., Chvatal, A., 2009. Differential calcium signalling in neuronal-glial networks. Front Biosci (Landmark Ed) 14, 2004-2016.

Verkhratsky, A., Sofroniew, M.V., Messing, A., deLanerolle, N.C., Rempe, D., Rodriguez, J.J., Nedergaard, M., 2012. Neurological diseases as primary gliopathies: a reassessment of neurocentrism. ASN Neuro 4.

Verkman, A.S., Ruiz-Ederra, J., Levin, M.H., 2008. Functions of aquaporins in the eye. Prog Retin Eye Res 27, 420-433.

Wang, J., Xu, X., Elliott, M.H., Zhu, M., Le, Y.Z., 2010. Muller cell-derived VEGF is essential for diabetes-induced retinal inflammation and vascular leakage. Diabetes 59, 2297-2305.

Yang, B., Verkman, A.S., 1997. Water and glycerol permeabilities of aquaporins 1-5 and MIP determined quantitatively by expression of epitope-tagged constructs in Xenopus oocytes. J Biol Chem 272, 16140-16146.

Figure legends

Figure 1: Analysis of intraretinal vasculature by isolectin staining in WT and AQP4 KO mice. A) Drawing of mouse retina highlighting the relationship between the intraretinal vasculature and glial cells. In red are shown the superficial (primary), the intermediate (inner deeper) and deep (outer deeper) plexi. The superficial plexus in mouse retina is localised at the NFL/GCL interface while the intermediate and deep plexi are at the IPL and OPL, respectively. Note that the superficial plexus is mainly ensheathed by astrocytes (green cells) while the intermediate and deep plexi are ensheathed by Müller cells (blue cells). (NFL, Nerve Fibre Layer; GCL, Ganglion Cell Layer; IPL, Inner Plexiform Layer; INL, Inner Nuclear Layer; OPL, Outer Plexiform Layer; ONL, Outer Nuclear Layer). B) xy confocal microscopy images of superficial, intermediate and deep plexi stained with anti-GFAP (blue) and anti-AQP4 (red) antibodies and IB4 (green). Scale bar 50 µm. C) z-stack (24 µm) image showing GFAP, AQP4 and IB4 signal distribution within the thickness of the retina. The colour is representative of the depth of the immunofluorescence signal, from red (top) to blue (bottom). D) xy confocal microscopy analysis of superficial, intermediate and deep plexi of WT and AQP4 KO retinas stained with IB4. Scale bar 100 µm.

Figure 2: Analysis of AQP4 depending BRB functionality by Evans blue assay. A) Left, epifluorescence images of Evans blue injected WT and AQP4 KO retinas. Extravasations are highlighted by arrowheads. Right, histogram showing the number of extravasations measured in WT and AQP4 KO mice. Scale bar 50 µm (*P<0.001, n=12). Representative xz (B) and xy (C) confocal microscopy acquisitions from the experiments described in (A) for AQP4 KO retinas. Note that the main site of extravasations (white arrow) is the deep plexus. Scale bar 30 µm.

Figure 3: Immunofluorescence and Western blot analysis of Glutamine Synthetase expression in AQP4 KO retina. A) Representative epifluorescence images of Glutamine Synthetase (GS) expression (green) in retinal sections prepared from WT and AQP4 KO mice. Nuclei (DAPI, blue), AQP4 (red) and merge are shown. GS immunoreactivity in the AQP4 KO shows no evident changes in expression and distribution compared to WT. Scale bar 50 µm. B,C) Western blot (B) and histogram (C) showing GS expression and densitometry analysis in WT and AQP4 KO mouse retina. GAPDH was used as an internal control for protein loading (n=8).

Figure 4: Immunofluorescence, Western blot and qPCR analysis of GFAP expression in AQP4 KO retina. A) Representative epifluorescence images of GFAP expression (green) in retinal sections prepared from WT and AQP4 KO mice. Nuclei (DAPI, blue), AQP4 (red) and merge are shown. Scale bar 50 µm. B) Draw of the three GFAP isoforms (α, δ, and k) analysed by Western blot (C, D) and qPCR (E). The red asterisk in exon-7 shows the epitope for the anti-GFAP G-A-5 monoclonal antibody used. C) Western blot showing GFAPα, δ and k isoform expression in WT and AQP4 KO mouse retina. Actin was used as an internal control for protein loading. D) Histograms summarizing the actin normalized densitometry analysis of single GFAP isoforms (α, δ, and k) or total GFAP (TOT) E) Histograms showing GFAPα, δ, and k mRNA levels detected by qPCR. Results are reported as GAPDH-normalized AQP4 KO /WT (*P<0.05, **P<0.005, ***P<0.0005; n=8 and n=3 for experiments shown in panels D and E, respectively).

Figure 5: Analysis of GFAP expression in WT and AQP4 KO whole mount retina. Confocal microscopy analysis of GFAP (yellow) immunolocalization in WT and AQP4 KO mouse whole retina; in red the endothelial marker CD31. GFAP is over-expressed in AQP4 KO

superficial plexus while no alterations were found at the level of the intermediate or deep plexus. Scale bar 50 µm.

Figure 6: Analysis of AQP4 and GFAP expression in AQP4 siRNA treated primary astrocyte cultures. Western blot showing AQP4 and GFAP expression in rat and mouse astrocytes treated with CTRL and AQP4 siRNA. No GFAP alteration was observed after ten days of AQP4 siRNA treatment either in rat or in mouse astrocytes. GAPDH was used as an internal control for protein loading (n=8).

Figure 7: mRNA increased expression of inflammatory markers in the retina of AQP4 KO mice**.** Scatter plot showing Tumor Necrosis Factor-α (TNF-α), Intercellular Adhesion Molecule1 (ICAM-1), Interleukin-1β (IL-1β) and Interleukin-6 (IL-6) mRNA levels in retinas of WT and AQP4 KO mice (*P<0.05, **P<0.005, ***P<0.0005; n=7).

Glio-vascular modifications caused by Aquaporin-4 deletion in the mouse retina

Grazia Paola Nicchia[a, b, °,*], Francesco Pisani[a,°], Laura Simone[c], Antonio Cibelli[a], Maria Grazia Mola[a], Massimo Dal Monte[d], Antonio Frigeri[b,e], Paola Bagnoli[d], Maria Svelto[a,f,g]

[a]Department of Bioscience, Biotechnologies and Biopharmaceutics and Centre of Excellence in Comparative Genomics, University of Bari "Aldo Moro", 70126 Bari, Italy.
[b]Department of Neuroscience, Albert Einstein College of Medicine, New York, Bronx, NY, USA.
[c]IRCCS "Casa Sollievo della Sofferenza", Research Hospital, San Giovanni Rotondo, Italy.
[d]Department of Biology, University of Pisa, 56127, Pisa, Italy.
[e]School of Medicine: Basic Medical Sciences, Neuroscience and Sense Organs, University of Bari "Aldo Moro", 70126 Bari, Italy.
[f]Institute of Biomembranes and Bioenergetics, National Research Council, Via Amendola 165/A, 70126 Bari, Italy.
[g]National Institute of Biostructures and Biosystems (INBB), Viale Medaglie D'Oro 305, 00136 Rome, Italy.

°G.P. Nicchia and F. Pisani equally contributed to the study.

Corresponding author: *Grazia Paola Nicchia, Department of Bioscience, Biotechnologies and Biopharmaceutics and Centre of Excellence in Comparative Genomics, University of Bari "Aldo Moro", Bari, Italy. Tel: +39 080 5443335; Fax: +39 080 5443388; Email: graziapaola.nicchia@uniba.it*

Abbreviations: AQP4, Aquaporin-4; KO, knockout; WT, Wild-type; BRB, blood-retinal barrier; KD, knockdown; GFAP, Glial Fibrillary Acid Protein; qPCR, quantitative polymerase chain reaction; TNF-α, Tumor necrosis factor-α; IL-6, Interleukin-6; IL-1β, Interleukin 1β; ICAM-1, Intercellular adhesion molecule1; siRNA, small interfering RNA; CNS, Central Nervous System; BBB, blood-brain barrier; NFL, Nerve Fibre Layer; RGC, Retinal Ganglion cell; C-terminal, carboxyl-terminal; NMO, Neuromyelitis Optica; IgG, Immunoglobulin G; NFL, Nerve Fibre Layer; CD-31, Cluster of Differentiation; GAPDH, Glyceraldehyde 3-phosphate dehydrogenase; HRP, horseradish peroxidase; GS, Glutamine Synthetase; VEGF, vascular endothelial growth factor; IPL, Inner Plexiform Layer; INL, Inner Nuclear Layer; OPL, Outer Plexiform Layer; ONL, Outer Nuclear Layer.

ABSTRACT

Aquaporin-4 (AQP4) is the Central Nervous System water channel highly expressed at the perivascular glial domain. In the retina, two types of AQP4 expressing glial cells take part in the blood-retinal barrier (BRB), astrocytes and Müller cells. The aim of the present study is to investigate the effect of AQP4 deletion on the retinal vasculature by looking at typical pathological hallmark such as BRB dysfunction and gliotic condition.

AQP4 dependent BRB properties were evaluated by measuring the number of extravasations in WT and AQP4 KO retinas by Evans blue injection assay. AQP4 deletion did not affect the retinal vasculature, as assessed by Isolectin B_4 staining, but caused BRB impairment to the deep plexus capillaries while the superficial and intermediate capillaries were not compromised. To investigate for gliotic responses caused by AQP4 deletion, Müller cells and astrocytes were analysed by immunofluorescence and western blot, using the Müller cell marker Glutamine Synthetase (GS) and the astrocyte marker GFAP. While GS expression was not altered in AQP4 KO retinas, a strong GFAP upregulation was found at the level of AQP4 KO astrocytes at the superficial plexus and not at Müller cells at the intermediate and deep plexi. These data, together with the upregulation of inflammatory markers (TNF-α, IL-6, IL-1β and ICAM-1) in AQP4 KO retinas indicated AQP4 deletion as responsible for a gliotic phenotype. Interestingly, no GFAP altered expression was found in AQP4 siRNA treated astrocyte primary cultures. All together these results indicate that AQP4 deletion is directly responsible for BRB dysfunction and gliotic condition in the mouse retina. The selective activation of glial cells at the primary plexus suggests that different regulatory elements control the reaction of astrocytes and Müller cells. Finally, GFAP upregulation is strictly linked to gliovascular crosstalk, as it is absent in astrocytes in culture. This study is useful to understand the role of AQP4 in the perivascular domain in the retina and its possible implications in the pathogenesis of retinal vascular diseases and of Neuromyelitis Optica, a human disease characterized by anti-AQP4 auto-antibodies.

Keywords: Aquaporin-4, Retina, Neuromyelitis Optica, Gliovascular biology, Blood-Retinal Barrier, Intraretinal Vasculature, Astrocytes, Müller cells.

1. Introduction

Aquaporins are water channel proteins conferring a faster water flux to several cell plasma membranes in the presence of osmotic and hydrostatic gradients (Yang and Verkman, 1997). Aquaporin-4 (AQP4) is the Central Nervous System (CNS) water channel, which is highly concentrated at the perivascular glial end-feet and takes part in the blood-brain barrier functional unit (Amiry-Moghaddam et al., 2003; Frigeri et al., 1995; Nicchia et al., 2008).

In the retina, two types of AQP4 expressing glial cells take part in the blood-retinal barrier (BRB), astrocytes and Müller cells (Newman, 2001). Astrocyte end-feet control the barrier properties only at the level of the superficial plexus whereas Müller cell end-feet do so also at the level of intermediate and deep plexus. Müller cells generated inside the retina span into its entire thickness providing structural and functional support to neurons (Newman and Reichenbach, 1996). AQP4 would here control the osmotic imbalance caused by the high neuronal activity (Goodyear et al., 2009). The relationship between AQP4 and the Kir4.1 potassium channel in Müller cells in the control of potassium homeostasis (Bosco et al., 2005; Nagelhus et al., 1999) is considered the reason for the impaired light-neuronal signal transduction reported for AQP4 KO mouse retina (Li et al., 2002). Astrocytes are stellate, without orientation, enter the retina from the brain along the developing optic nerve (Stone and Dreher, 1987) and form a homogeneous plexus on the Nerve Fibre Layer (NFL) and Retinal Ganglion cell (RGC) layer. Astrocytes here play a key role in maintaining either the BRB properties or the survival of RGC, whose axons form the optic nerve. Though the role of AQP4 in maintaining water homeostasis in Müller cells has been extensively studied (Goodyear et al., 2009; Verkman et al., 2008), less attention has been paid to addressing its function under

normal conditions in the perivascular glial domain. Both Müller cells and astrocytes are enriched in intermediate filaments, however, Glial Fibrillary Acid Protein (GFAP) is the major component of the filaments in astrocytes (Dixon and Eng, 1981; Eng, 1985) but is found at very low levels in Müller cells (Bignami and Dahl, 1979). GFAP is thought to provide astrocytes with mechanical force as well as a particular shape, especially at the level of the terminal endfeet (Hyder et al., 2011). Several GFAP isoforms exist (Kamphuis et al., 2012), the canonical GFAP isoform is α, which is able to assemble in filaments based on a C-terminal motif that is instead absent in GFAPδ and κ, destabilizing the filaments (Blechingberg et al., 2007a; Hol and Pekny, 2015; Kamphuis et al., 2012).

BRB dysfunction and glial activation are key pathological features in a number of retinal vascular diseases, such as retinopathy of prematurity, diabetic retinopathy, and branch retinal vein occlusion, considered a primary cause of visual impairment and blindness (Coorey et al., 2012). Interestingly, altered AQP4 expression is also associated with some of these pathologies, such as branch retinal vein occlusion (Koferl et al., 2014) and diabetic retinopathy (Kumar et al., 2014; Qin et al., 2012). In diabetic rats, AQP4 knockdown (KD) leads to exacerbation of retinopathy with BRB dysfunction and inflammatory response (Cui et al., 2012). In Neuromyelitis Optica (NMO), a CNS autoimmune inflammatory “aquaporinopathy” affecting the optic nerve and spinal cord (Bergamaschi and Ghezzi, 2004; Jarius and Wildemann, 2010; Lennon et al., 2005; Lennon et al., 2004) and leading to paralysis and blindness, AQP4 is the molecular target of the autoantibody NMO IgG, the pathological hallmark of the disease. Interestingly, optic neuritis in NMO patients is characterized by retinal modifications at the vascular level and on the NFL (Camicione et al., 2010; Green and Cree, 2009; Merle et al., 2008), most likely caused by NMO IgG binding to AQP4 expressing cells in the retina and optic nerve.

Understanding the molecular basis of the role played by AQP4 at the level of retinal vasculature is fundamental for clarifying the pathogenesis of the diseases involving AQP4 dependent alterations in the retinal vasculature. Moreover, it will help in elucidating the role that glial cells play in the pathogenesis of such diseases, therefore supporting the developing of novel therapies. The aim of the present study is to investigate the effect of AQP4 deletion on the retinal vasculature by looking at typical pathological hallmark such as BRB dysfunction and gliotic condition.

2. Materials and Methods

2.1 Animals

5-10 month old AQP4 KO mice with a CD1 genetic background (Basco et al., 2013) and age matched controls were used. CD1 mice and Wistar rats were used for astrocyte primary cultures. Experiments were performed in accordance with the ARVO Statement for the Use of Animals in Ophthalmic and Vision Research and in compliance with the Italian law on animal care (Italian Health Department Approved Project n°100/2014-B). All experiments were designed to minimize the number of animals used and their suffering. The mice used here were bred in the approved facility at the University of Bari.

2.2 Antibodies

The following primary antibodies were used: goat polyclonal anti-AQP4 (Santa Cruz, CA, USA); goat polyclonal anti-CD31 (Santa Cruz, CA, USA); rabbit polyclonal anti-GFAP (Sigma-Aldrich, Milan, Italy); mouse monoclonal anti-GFAP (clone G-A-5, Millipore, Merck KGaA, Darmstadt, Germany); mouse monoclonal anti-GAPDH (MAB 374, Millipore, Merck KGaA, Darmstadt, Germany); mouse monoclonal anti-Glutamine Synthetase (MAB 302, Millipore, Merck); goat polyclonal anti-actin (Santa Cruz, CA, USA). The following secondary antibodies (all from Invitrogen, Milan, Italy) were used for immunofluorescence: donkey anti-goat Alexa Fluor488; donkey anti-mouse Alexa Fluor488; donkey anti-rabbit Alexa Fluor594; donkey anti-goat Alexa Fluor594; donkey anti-rabbit Alexa Fluor647. The following secondary antibodies (all from Santa Cruz, CA, USA) were used for Western blot:

goat anti-mouse IgG-horseradish peroxidase (HRP); goat anti-rabbit IgG-HRP; donkey anti-goat IgG-HRP.

2.3 Astrocyte primary cultures and RNA interference

Astrocytes were prepared from primary cell cultures of neocortical tissues as previously described (Nicchia et al., 2003). RNA interference experiments were performed as follows: astrocytes were transfected with 100 nM AQP4 siRNA smart pool or scrambled siRNA (Nicchia et al., 2003) by oligofectamine (Invitrogen, Milan, Italy), in a 24 multi-well format, according to the instruction manual, using high glucose GlutaMAX™ DMEM (Invitrogen, Milan, Italy), supplemented with 10% FBS (Invitrogen, Milan, Italy). After 10 days, cells were lysed with 100 µl of RIPA Buffer (see paragraph "western blot" for composition), and total protein content was measured using the Micro-BCA Protein Assay Kit (Thermo Scientific, Rockford, IL, USA). Five µl of proteins were analyzed by Western blot as later described.

2.4 Preparation of whole-mount retinas and retinal sections for immunofluorescence and Isolectin B_4 staining

Wild type (WT) and AQP4 KO mice were anesthetized by intraperitoneal injection of urethane (1.2 g/kg body weight). Retinas were explanted in ice cold PBS, washed several times and fixed with 4% paraformaldehyde (Sigma-Aldrich, Milan, Italy) for 60 min. For Isolectin staining, retinas were permeabilized overnight with 0.5% Triton X-100 in PBS, washed several times in PBS and incubated overnight with 10 µg/ml of FITC-conjugated Isolectin B_4 (IB4) from Bandeiraea simplicifolia (Griffonia simplicifolia). After washings in PBS, retinas were finally mounted in PBS-glycerol

(1:1) pH 8.0, containing 1% n-propyl gallate. For immunofluorescence, after fixation retinas were washed in PBS, permeabilized with 0.5% Triton X-100 in PBS for 30 min and saturated for 30 min with 1% BSA, 0.5% Triton X-100 in PBS. All these steps were performed at RT. Retinas were incubated with primary antibodies for 48h at 4°C in 1% BSA in PBS, washed three times with 1% BSA, 0.5% Triton X-100 in PBS for 20 min each and then incubated with secondary antibodies (1:1000 dilution) and isolectin B_4 (10 µg/ml) for 24 h in the same solution at 4°C. The day after, the retinas were washed three times in PBS, and finally mounted in PBS-glycerol (1:1) pH 8.0, containing 1% n-propyl gallate. For section preparation, enucleated eyes were fixed in 4% PFA solution for 2-3 hours at 4°C. After removal of cornea, iris and lens, whole posterior eyecups were immersed in 30% sucrose solution in PBS overnight; then, eyescups were embedded in OCT compound (Leica Biosystem, Nussloch, Germany) and immediately frozen at -80°C. Sections of 10-µm thickness were cut on a cryostat at -20°C. After blocking, sections were incubated with primary antibodies overnight at 4°C in blocking solution (0.1% Gelatin in PBS), washed for 30 min and then incubated with secondary antibodies for 1 h. Finally, the sections were washed for 30 min in PBS and mounted in PBS-glycerol (1:1) pH 8.0, containing 1% n-propyl gallate.

2.5 Confocal microscopy analysis

Confocal images were obtained with an automated inverted Leica TCS SP8 confocal microscope using a 16x and 63x HC PL Apo oil CS2 objective. 3D-images and projections from the z-stack were constructed and processed using Leica Application Suite X software.

2.6 Protein extraction from retinas, Western blot and densitometric analysis

Eyes were harvested from WT and AQP4 KO mice, and immediately dissected in ice cold PBS. Excessive liquid was removed, retinas snap-frozen in liquid nitrogen and stored at -80°C. Proteins were extracted from stored explanted retinas in 7-10 volumes of RIPA buffer (10 mM Tris-HCl, pH 7.4; 140 mM NaCl; 1% Triton X-100; 1% Na deoxycholate; 0.1% SDS; 1 mM Na_3VO_4; 1 mM NaF and 1 mM EDTA) added with a cocktail of protease inhibitors (Roche, Milan, Italy). The lysis was performed on ice for 1h and the samples were then centrifuged at 22,000xg for 1h. The protein content of the supernatant was measured with a bicinchoninic acid (BCA) Protein Assay Kit (Pierce, Rockford, IL, USA). 30 µg of protein samples was loaded in NuPAGE 4-12% Bis-Tris Gel (Invitrogen, Milan, Italy) and transferred to polyvinylidene difluoride membranes (Millipore, Milan, Italy), as described previously (Pisani et al., 2014). Membranes with blotted proteins were incubated with primary antibodies, washed, and incubated with peroxidase-conjugated secondary antibodies (Nicchia et al., 2003). Reactive proteins were revealed using an enhanced chemiluminescent detection system (ECL Plus, Thermo scientific, Rockford, IL, USA) and visualized on a Versadoc imaging system (BioRad, Milan, Italy). Densitometry analysis was performed using ImageJ Software (National Institute of Mental Health, Bethesda, Maryland, USA) and analyzed by GraphPad Prism 5 (GraphPad, San Diego, USA).

2.7 qPCR

RNA extraction was carried out using Trizol Reagent (Invitrogen, Milan, Italy) according to the instruction manual. Total RNA was quantified by Nanodrop

(Thermo scientific, Waltham, MA, USA). 3 µg of total RNA were retrotranscribed by SuperScript III Reverse Transcriptase (Invitrogen, Milan, Italy). GFAP isoform expression was measured by the GAPDH normalized ΔΔCt quantification method using previously published primers (Kamphuis et al., 2012). Sybr Green (Invitrogen, Milan, Italy) and StepOne (Applied Biosystems) were used. Instead, the expression of Tumor necrosis factor-α (TNF-α), Intercellular adhesion molecule1 (ICAM-1), Interleukin (IL)-1β and IL-6 was measured by the Rpl13a normalized ΔΔCt quantification method using previously published primers (Dal Monte et al., 2015).

2.8 Evans Blue assay

Mice retinal blood vessel permeability was tested by Evans Blue assay as follows: 300µl of Evans Blue (30 mg/ml) in PBS was intraperitoneally injected. After 20 min, retinas were explanted and extravasation evaluated by epifluorescence analysis at an excitation wavelength of 594nm with a Leica DM RXA microscope using a 16x oil PL FL FLUOTAR objective. Five digital images from each quadrant for each retina were recorded and processed using Las AF software and the number of extravasations manually counted.

2.9 Statistical analysis

Mean ± standard error is reported in the results. Statistical analysis was performed using GraphPad Prism 5 (GraphPad, San Diego, USA) by ANOVA or t-test for unpaired data. A p value < 0.05 was considered statistically significant.

3. Results

3.1 Impaired BRB functionality at the AQP4 KO deep plexus

The relationship between the intraretinal vasculature and macroglial cells is shown in Fig. 1A. The drawing shows that the superficial plexus is ensheathed by glial cell processes arising mainly from astrocytes while the intermediate and deep plexi are ensheathed by glial processes arising from Müller cells. To analyze AQP4 expression at the gliovascular interface, confocal microscopy experiments were performed on the whole retina, using the astrocyte marker GFAP and IB4 to stain the retinal vasculature (Fig. 1B, C). At the superficial plexus, GFAP expression at the level of astrocytes was very strong, as expected. AQP4 staining was here concentrated at the perivascular level but there was also AQP4 signal coming from Muller cells processes uniformly distributed within the layer under analysis. GFAP staining was found to be very low at the intermediate and the deep plexi, the glial part here being represented by Müller cells. The capillaries here appeared to be very well depicted by AQP4 staining, indicating very highly concentrated AQP4 expression in the perivascular glial processes (Fig. 1B). Fig. 1C shows a z-stack distribution of GFAP, AQP4 and IB4 expression depending on the depth of the whole retina analysed by confocal microscopy. This analysis highlights that GFAP signal is concentrated at the superficial plexus while AQP4 and IB4 overlap at the three plexi, indicating that intraretinal vasculature is completely ensheathed by glial processes with highly enriched AQP4 water channels. AQP4 concentrated fluorescence at the deep plexus corresponds to its high expression at Muller cells.

To investigate whether AQP4 KO mice are characterized by intraretinal vascular abnormalities, confocal microscopy analysis was performed on WT and AQP4 KO

retinas stained with IB4. Separate images, acquired for each plexus (Fig. 1D) revealed no differences, indicating that AQP4 deletion does not cause intaretinal structural alteration at the vascular level.

AQP4 dependent BRB properties were then evaluated by measuring the number of extravasations in WT and AQP4 KO retinas by Evans blue injection assay. Treated retinas were isolated and analysed by epifluorescence (Fig. 2A) and confocal microscopy (Fig. 2B-C). Epifluorescence analysis, performed to quantify the number of extravasations, allowed us to associate a statistically significant higher number of extravasations to AQP4 KO retinas (Fig. 2A). By confocal microscopy, the extravasations were localized at the deep plexus capillaries while the superficial and intermediate plexus were not compromised (Fig. 2B,C). These data point to AQP4 absence being responsible for functional alterations at the BRB level, which are evident at the deep plexus, where AQP4 is highly concentrated.

3.2 Muller cells, identified by Glutamine Synthetase expression, do not show alterations in the retina of AQP4 KO mice

In order to investigated gliotic responses caused by AQP4 deletion in the retina, Müller cells and astrocytes were analysed by immunofluorescence on retinal sections and western blot, using the Muller cell marker Glutamine Synthetase (Fig. 3) and the astrocyte marker GFAP (Fig. 4). We observed that pattern and intensity of GS immunoreactivity was not altered in the absence of AQP4 (Fig. 3A), in line with WB results showing comparable GS expression level between WT and AQP4 KO retinas (Fig. 3B,C). These results indicate the absence of a major impact of AQP4 deletion on retinal Muller cells.

3.3 Reactive phenotype of AQP4 KO superficial plexus assessed by strong GFAP upregulation

The hypothesis of a gliotic phenotype to explain structural alterations at AQP4 KO gliovascular interface was also investigated by the analysis of GFAP expression by immunolocalization on cryosectioned retinas and whole-mount retina, by Western blot and qPCR (Fig. 4, Fig.5). GFAP immunolocalization on retinal sections (Fig. 4A) showed a grossly comparable GFAP distribution between WT and AQP4 KO retinas although the signal appeared stronger in AQP4 KO ones. For Western blot, the analysis was carried out to discriminate between the relative expression of the most characterized GFAP isoforms, GFAPα, δ, and κ. To this end, a monoclonal antibody (clone G-A-5), able to selectively recognize these isoforms, was used (Fig. 4B). Western blot results revealed that all the GFAP isoforms were significantly upregulated in AQP4 KO vs WT (Fig. 4 C,D). Finally, the quantitative analysis of gene expression demonstrated mRNA level of GFAPα and GFAPδ increase of 2 fold in the AQP4 KO mice compared with WT mice, while mRNA expression level of GFAPκ showed a 10 fold increase (Fig. 4 E). The results obtained for GFAP at the mRNA level were in line with those obtained for GFAP protein with a particular upregulation of GFAPκ.

GFAP upregulation in AQP4 KO was then more deeply investigated by confocal microscopy on whole mount retinas (Fig. 5). Immunofluorescence results revealed a strong GFAP overexpression only at the level of the AQP4 KO superficial plexus. No GFAP upregulation was detected at the intermediate or deep plexi.

Altogether, these data indicate that a gliotic phenotype, with a GFAP upregulation, is selectively acquired by AQP4 KO astrocytes at the superficial plexus and not by Müller cells at the intermediate and deep plexi.

3.4 AQP4 KD does not alter GFAP expression in astrocyte primary cultures

The direct cause-effect relationship between AQP4 deletion and the altered expression of GFAP isoforms observed in AQP4 KO retinas was then investigated in a cell culture system outside the gliovascular environment (Fig. 6). We decided to take advantage of primary astrocyte cultures characterized by AQP4 reduced expression, such as AQP4 KD astrocytes obtained by RNA interference (Nicchia et al., 2005). By Western blot, we analysed GFAP expression in rat and mouse primary culture of astrocytes treated with specific AQP4 siRNA for 10 days and no difference was found, GFAPα being the only isoform expressed. These data demonstrate that loss of AQP4 expression is not a direct cause of GFAP alterations outside the gliovascular environment.

3.5 Inflammatory pattern in AQP4 KO retinas

The inflammatory state of AQP KO retinas was analysed (Fig. 7) by measuring the level of proinflammatory cytokines such as IL-1β, IL-6, TNF-α and the intercellular adhesion molecule (ICAM-1), this last being upregulated following exposure to proinflammatory stimuli such as TNF-α and IL-1β (Eddleston and Mucke, 1993). Quantitative analysis of gene expression by qPCR demonstrated that mRNA level of IL-1β and TNF-α increased around 3 folds in AQP4 KO compared to WT while

mRNA expression level of IL-6 increased 7 folds and of ICAM-1 2 folds. These data indicate that AQP4 absence in the retina is responsible for an inflammatory status.

4. Discussion

The breakdown of BRB is a common feature of several retinal vascular diseases and it is often associated with an inflammatory response (Coorey et al., 2012). We here show that AQP4 deletion causes BRB extravasations exclusively localized at the deep plexus of the retina where normally AQP4 is very highly concentrated. A possible explanation for the difference in BRB extravasation is that the deep plexus smaller calibre vessels, being more fragile, become more susceptible to BRB dysfunction in the absence of AQP4. We cannot exclude however, that AQP4 deletion may cause a polarized release of paracrine factors responsible for the increase in BRB permeability. For instance, AQP4 KD in cultured rat Müller cells enhances the release of vascular endothelial growth factor (VEGF) (Shelton et al., 2009), and it has been demonstrated that Müller cell-derived VEGF plays an essential and causative role in vascular lesions and vascular leakage in diseased retinas (Wang et al., 2010). Interestingly, pathological conditions, such as diabetic retinopathy (Kumar et al., 2014; Qin et al., 2012), as well as transient retinal ischemia (Hirrlinger et al., 2010; Koferl et al., 2014) and retinal injury (Dibas et al., 2008; Iandiev et al., 2008) are characterized by BRB dysfunctions and by an altered expression of both AQP4 and GFAP (Cui et al., 2012). The hypothesis of a gliotic condition, as a consequence of AQP4 deletion, was therefore investigated. GFAP, normally used to identify astrocytes in the CNS, is also a very well known marker of active gliosis, being upregulated after traumatic injury and neuronal degeneration. In the retina, under normal conditions, it is expressed by astrocytes, and at a very low level by Müller cells. However, it is has been reported that, in response to retinal injury or photoreceptor degeneration, GFAP expression is activated in Müller cells and becomes a marker of retinal gliosis (Ekstrom et al., 1988). Interestingly, there is

a study by Verderber et al., (Verderber et al., 1995) reporting that regulatory elements, which determine GFAP induction in Müller cells, are different from those involved in GFAP expression in astrocytes. We here show that AQP4 deletion causes a strong upregulation of GFAP at the perivascular astrocytes of the superficial layer and not at perivascular Müller cells at the intermediate and deep plexi. This data, here supported by the altered inflammatory pattern found in AQP4 KO retinas, strongly indicates a gliotic condition primarily affecting the GCL.

The function of reactive gliosis and, in particular, whether it is pathological or beneficial is still controversial (Verkhratsky et al., 2012). We here show BRB impairment at the deep plexus, which is not interested by a gliotic condition and, viceversa, BRB integrity at the superficial plexus where a gliotic condition is identified by GFAP upregulation. This scenario could be considered an example of gliosis as a “beneficial reaction” occurring at the superficial plexus with the aim to protect the integrity of the BRB. In line with this view, we can further speculate that the absence of glial activation at the deep plexus is one of the causes for the impaired BRB observed.

AQP4 KO retinas have been previously analysed by Li et al. (2002) and no difference in ultrastructure was reported but a mild impaired retinal function was found (Li et al., 2002). However, a more recent study by Pannicke et al (Pannicke et al., 2010), performed on the same AQP4 KO mice used by Li et al (2002), shows that deletion of AQP4 is associated with a distinct inflammatory response of the retina, which is in agreement with our results. The same study, however, reported a significant reduction in GFAP mRNA in AQP4 KO retinas while GFAP protein expression, evaluated by immunolocalization, was not altered. Although, protein levels cannot be accurately determined by immunofluorescence and no WB were performed in the study by Li, the unaltered GFAP protein expression could be

explained because the analysis by immunofluorescence was carried out on cross sections showing the retinal layers, not as informative for astrocyte details as by longitudinal analysis showing each plexus. It is more difficult to explain the discrepancy between the reduced GFAP mRNA expression with the significant increase here shown instead. Although, in general, reduced mRNA expression not followed by a parallel decrease in the relative protein expression does not have a physiological significance, the only explanations for such a discrepancy are either the mouse model used or the age of the animals. Differences in the phenotype of these mice (Owler et al., 2010), unrelated with AQP4, could be at the base of the discrepancy on GFAP mRNA levels in AQP4 KO mice. Alternatively, this difference could be ascribable to the use of younger mice (3-4 months old) by Pannicke. Future study will be focused on age dependent alteration of GFAP mRNA and protein in AQP4 KO mice. However, we believe it is important to highlight that, independently of the up or down regulation of GFAP mRNA, and despite phenotype differences, an altered inflammation pattern is observed in both mouse models.

Considering that reactive astrocytes in the retina lead to RGC death and contribute to visual impairment (Ganesh and Chintala, 2011), we can here propose that the impaired retinal function found in AQP4 KO mice (Li et al., 2002), so far attributed only to Müller cell alteration, can also be ascribed to the presence of an inflammatory response of the superficial plexus, causing neuronal damage and optic nerve impairment. Moreover, AQP4 deletion as the cause of GFAP upregulation in retinal astrocytes and not in Müller cells is a further support for differential regulatory elements being involved in the activation of the two types of macroglial cells (Verderber et al., 1995).

While GFAPα is the canonical isoform characteristic of healthy glial cells (Kamphuis et al., 2012; Moeton et al., 2014), isoforms δ and κ are differentially expressed in

pathological conditions. In particular, GFAPk is increased in multiform glioblastoma (Blechingberg et al., 2007a; Blechingberg et al., 2007b). Our data show a particular upregulation of GFAPk mRNA in AQP4 KO retina, in line with the observed pathological signs.

AQP4 deletion as the direct cause of a GFAP altered expression has been also investigated here using primary astrocyte cultures lacking AQP4, in particular, AQP4 siRNA treated astrocytes (Nicchia et al., 2003). We show that AQP4 KD in culture is not sufficient to produce any alteration in GFAP isoform expression even if the KD is prolonged by up to ten days. Therefore, we can conclude that AQP4 absence in cultured astrocytes does not cause a gliotic phenotype, which seems strictly dependent on a glio-vascular crosstalk. This result may find an explanation on the basis of the culture conditions of astrocytes outside their own *in vivo* environment in which AQP4 expression is maintained but its typical polarized expression is lost, the water flux being strictly linked to the transport of molecules and ions normally occurring at the perivascular glial processes (Nicchia et al., 2000). On the basis of the evidence from studies on astrocytes in cultures, we can assume that the inflammatory condition, indicated by GFAP upregulation and by the upregulation of the inflammatory markers, is strictly linked to a gliovascular expression of AQP4.

During pathological situations in the CNS, such as cerebral ischemia, a rapid intracellular calcium increase triggers reactive gliosis (Verkhratsky et al., 2009). Interestingly, synergic cooperation between AQP4 and the polymodal transient receptor potential vanilloid 4 (TRPV4) channel has been proposed, in controlling calcium homeostasis in astrocytes (Benfenati et al., 2011; Mola et al., 2016) and Müller cells (Jo et al., 2015). In particular, the mechanisms proposed by Jo et al. and Mola et al. are very similar in highlighting a functional, rather than physical,

interaction, strictly linked to the effect of AQP-dependent fast water flux on the level of plasma membrane stretch and therefore on TRPV4 activation. We can speculate that a physiological diversity between astrocytes and Müller cells in sensing and modulating calcium homeostasis and in controlling the downstream mechanism involved in calcium dependent gliosis, can be at the base of their different reaction to AQP4 deletion.

5. Conclusion

In conclusion, we here show that AQP4 deletion causes BRB dysfunction at the deep plexus, an inflammatory status and a reactive phenotype, most likely beneficial, restricted to the superficial plexus with GFAP upregulation. The possibilities are: 1) The altered water homeostasis caused by AQP4 deletion is the direct cause of both BRB impairment and astrocyte activation. If this is the case, the AQP4 dependent reactive condition would be strictly linked to gliovascular crosstalk, which is absent when astrocytes are placed in culture; 2) AQP4 deletion causes BRB dysfunction in turn causing an astrocyte reaction. In this case, the GFAP upregulation found would be the consequence of extravasation of fluid and inflammatory factors, causing the inflammatory response. The reason why, however, those factors would act only on astrocytes and not on Müller cells would be unclear; 3) AQP4 deletion is a direct cause of astrocyte activation with an inflammatory response in turn responsible for BRB impairment.

We believe this study adds knowledge on the modification occurring in the absence of AQP4 useful in understanding its role in retinal glial cells under normal conditions and helps in elucidating the molecular basis leading to BRB breakdown and glial activation in the retina. Moreover, it provides important pieces of information on the

role that AQP4 may play in the pathogenesis of retinal vascular diseases, such as such as branch retinal vein occlusion and diabetic retinopathy and NMO. In particular, in future studies, it will be important to address whether BRB impairment and/or an inflammatory response are involved in optic neuritis caused by NMO IgG binding to AQP4 expressing glial cells in NMO patients.

Acknowledgments

The authors would like to thank Richard Lusardi for his assistance in revising the English of the article, Gaetano De Vito for his excellent technical assistance, and Francesca Sanarica for her support in retinal explantation and technical assistance.

This study was financed by the Italian Ministry of University and Research (Project Firb “Futuro in Ricerca” RBFR12SJA8 to Grazia Paola Nicchia) and by the Italian Ministry of Health 2014-2017 (Project Biomedical RF-2011-02351158 to Paola Bagnoli).

References

Amiry-Moghaddam, M., Otsuka, T., Hurn, P.D., Traystman, R.J., Haug, F.M., Froehner, S.C., Adams, M.E., Neely, J.D., Agre, P., Ottersen, O.P., Bhardwaj, A., 2003. An alpha-syntrophin-dependent pool of AQP4 in astroglial end-feet confers bidirectional water flow between blood and brain. Proc Natl Acad Sci U S A 100, 2106-2111.

Basco, D., Blaauw, B., Pisani, F., Sparaneo, A., Nicchia, G.P., Mola, M.G., Reggiani, C., Svelto, M., Frigeri, A., 2013. AQP4-Dependent Water Transport Plays a Functional Role in Exercise-Induced Skeletal Muscle Adaptations. PLoS One 8, e58712.

Benfenati, V., Caprini, M., Dovizio, M., Mylonakou, M.N., Ferroni, S., Ottersen, O.P., Amiry-Moghaddam, M., 2011. An aquaporin-4/transient receptor potential vanilloid 4 (AQP4/TRPV4) complex is essential for cell-volume control in astrocytes. Proc Natl Acad Sci U S A 108, 2563-2568.

Bergamaschi, R., Ghezzi, A., 2004. Devic's neuromyelitis optica: clinical features and prognostic factors. Neurol Sci 25 Suppl 4, S364-367.

Bignami, A., Dahl, D., 1979. The radial glia of Muller in the rat retina and their response to injury. An immunofluorescence study with antibodies to the glial fibrillary acidic (GFA) protein. Experimental eye research 28, 63-69.

Blechingberg, J., Holm, I.E., Nielsen, K.B., Jensen, T.H., Jorgensen, A.L., Nielsen, A.L., 2007a. Identification and characterization of GFAPkappa, a novel glial fibrillary acidic protein isoform. Glia 55, 497-507.

Blechingberg, J., Lykke-Andersen, S., Jensen, T.H., Jorgensen, A.L., Nielsen, A.L., 2007b. Regulatory mechanisms for 3'-end alternative splicing and polyadenylation of the Glial Fibrillary Acidic Protein, GFAP, transcript. Nucleic Acids Res 35, 7636-7650.

Bosco, A., Cusato, K., Nicchia, G.P., Frigeri, A., Spray, D.C., 2005. A developmental switch in the expression of aquaporin-4 and Kir4.1 from horizontal to Muller cells in mouse retina. Invest Ophthalmol Vis Sci 46, 3869-3875.

Camicione, P., Fodor, E., Pannarello, S., Barabino, S., 2010. Retinal peripapillary nerve fiber layer thickness in a 13-year-old boy with neuromyelitis optica. European journal of ophthalmology 20, 485-488.

Coorey, N.J., Shen, W., Chung, S.H., Zhu, L., Gillies, M.C., 2012. The role of glia in retinal vascular disease. Clinical & experimental optometry : journal of the Australian Optometrical Association 95, 266-281.

Cui, B., Sun, J.H., Xiang, F.F., Liu, L., Li, W.J., 2012. Aquaporin 4 knockdown exacerbates streptozotocin-induced diabetic retinopathy through aggravating inflammatory response. Exp Eye Res 98, 37-43.

Dal Monte, M., Rezzola, S., Cammalleri, M., Belleri, M., Locri, F., Morbidelli, L., Corsini, M., Paganini, G., Semeraro, F., Cancarini, A., Rusciano, D., Presta, M., Bagnoli, P., 2015. Antiangiogenic Effectiveness of the Urokinase Receptor-Derived Peptide UPARANT in a Model of Oxygen-Induced Retinopathy. Invest Ophthalmol Vis Sci 56, 2392-2407.

Dibas, A., Yang, M.H., He, S., Bobich, J., Yorio, T., 2008. Changes in ocular aquaporin-4 (AQP4) expression following retinal injury. Mol Vis 14, 1770-1783.

Dixon, R.G., Eng, L.F., 1981. Glial fibrillary acidic protein in the optic nerve of the developing albino rat: an immunoperoxidase study of paraffin-embedded tissue. The Journal of comparative neurology 201, 15-24.

Eddleston, M., Mucke, L., 1993. Molecular profile of reactive astrocytes--implications for their role in neurologic disease. Neuroscience 54, 15-36.

Ekstrom, P., Sanyal, S., Narfstrom, K., Chader, G.J., van Veen, T., 1988. Accumulation of glial fibrillary acidic protein in Muller radial glia during retinal degeneration. Investigative ophthalmology & visual science 29, 1363-1371.

Eng, L.F., 1985. Glial fibrillary acidic protein (GFAP): the major protein of glial intermediate filaments in differentiated astrocytes. Journal of neuroimmunology 8, 203-214.

Frigeri, A., Gropper, M.A., Umenishi, F., Kawashima, M., Brown, D., Verkman AS., 1995. Localization of MIWC and GLIP water channel homologs in neuromuscular, epithelial and glandular tissues. J Cell Sci 108, 2993-3002.

Ganesh, B.S., Chintala, S.K., 2011. Inhibition of reactive gliosis attenuates excitotoxicity-mediated death of retinal ganglion cells. PLoS One 6, e18305.

Goodyear, M.J., Crewther, S.G., Junghans, B.M., 2009. A role for aquaporin-4 in fluid regulation in the inner retina. Vis Neurosci 26, 159-165.

Green, A.J., Cree, B.A., 2009. Distinctive retinal nerve fibre layer and vascular changes in neuromyelitis optica following optic neuritis. Journal of neurology, neurosurgery, and psychiatry 80, 1002-1005.

Hirrlinger, P.G., Ulbricht, E., Iandiev, I., Reichenbach, A., Pannicke, T., 2010. Alterations in protein expression and membrane properties during Muller cell gliosis in a murine model of transient retinal ischemia. Neurosci Lett 472, 73-78.

Hol, E.M., Pekny, M., 2015. Glial fibrillary acidic protein (GFAP) and the astrocyte intermediate filament system in diseases of the central nervous system. Curr Opin Cell Biol 32, 121-130.

Hyder, C.L., Isoniemi, K.O., Torvaldson, E.S., Eriksson, J.E., 2011. Insights into intermediate filament regulation from development to ageing. J Cell Sci 124, 1363-1372.

Iandiev, I., Pannicke, T., Hollborn, M., Wiedemann, P., Reichenbach, A., Grimm, C., Reme, C.E., Bringmann, A., 2008. Localization of glial aquaporin-4 and Kir4.1 in the light-injured murine retina. Neurosci Lett 434, 317-321.

Jarius, S., Wildemann, B., 2010. AQP4 antibodies in neuromyelitis optica: diagnostic and pathogenetic relevance. Nature reviews. Neurology 6, 383-392.

Jo, A.O., Ryskamp, D.A., Phuong, T.T., Verkman, A.S., Yarishkin, O., MacAulay, N., Križaj, D., 2015. TRPV4 and AQP4 Channels Synergistically Regulate Cell Volume and Calcium Homeostasis in Retinal Müller Glia. J Neurosci 35, 13525-13537.

Kamphuis, W., Mamber, C., Moeton, M., Kooijman, L., Sluijs, J.A., Jansen, A.H., Verveer, M., de Groot, L.R., Smith, V.D., Rangarajan, S., Rodriguez, J.J., Orre, M., Hol, E.M., 2012. GFAP isoforms in adult mouse brain with a focus on neurogenic astrocytes and reactive astrogliosis in mouse models of Alzheimer disease. PLoS One 7, e42823.

Koferl, P., Hollborn, M., Rehak, J., Iandiev, I., Dukic-Stefanovic, S., Wiedemann, P., Kohen, L., Bringmann, A., Rehak, M., 2014. Effects of arteriolar constriction on retinal gene expression and Muller cell responses in a rat model of branch retinal vein occlusion. Graefes Arch Clin Exp Ophthalmol 252, 257-265.

Kumar, B., Gupta, S.K., Nag, T.C., Srivastava, S., Saxena, R., Jha, K.A., Srinivasan, B.P., 2014. Retinal neuroprotective effects of quercetin in streptozotocin-induced diabetic rats. Exp Eye Res 125, 193-202.

Lennon, V.A., Kryzer, T.J., Pittock, S.J., Verkman, A.S., Hinson, S.R., 2005. IgG marker of optic-spinal multiple sclerosis binds to the aquaporin-4 water channel. J Exp Med 202, 473-477.

Lennon, V.A., Wingerchuk, D.M., Kryzer, T.J., Pittock, S.J., Lucchinetti, C.F., Fujihara, K., Nakashima, I., Weinshenker, B.G., 2004. A serum autoantibody marker of neuromyelitis optica: distinction from multiple sclerosis. Lancet 364, 2106-2112.

Li, J., Patil, R.V., Verkman, A.S., 2002. Mildly abnormal retinal function in transgenic mice without Muller cell aquaporin-4 water channels. Invest Ophthalmol Vis Sci 43, 573-579.

Merle, H., Olindo, S., Donnio, A., Richer, R., Smadja, D., Cabre, P., 2008. Retinal peripapillary nerve fiber layer thickness in neuromyelitis optica. Investigative ophthalmology & visual science 49, 4412-4417.

Moeton, M., Kanski, R., Stassen, O.M., Sluijs, J.A., Geerts, D., van Tijn, P., Wiche, G., van Strien, M.E., Hol, E.M., 2014. Silencing GFAP isoforms in astrocytoma cells disturbs laminin-dependent motility and cell adhesion. FASEB J 28, 2942-2954.

Mola, M.G., Sparaneo, A., Gargano, C.D., Spray, D.C., Svelto, M., Frigeri, A., Scemes, E., Nicchia, G.P., 2016. The speed of swelling kinetics modulates cell volume regulation and calcium signaling in astrocytes: A different point of view on the role of aquaporins. Glia 64, 139-154.

Nagelhus, E.A., Horio, Y., Inanobe, A., Fujita, A., Haug, F.M., Nielsen, S., Kurachi, Y., Ottersen, O.P., 1999. Immunogold evidence suggests that coupling of K+ siphoning and water transport in rat retinal Muller cells is mediated by a coenrichment of Kir4.1 and AQP4 in specific membrane domains. Glia 26, 47-54.

Newman, E., Reichenbach, A., 1996. The Muller cell: a functional element of the retina. Trends in neurosciences 19, 307-312.

Newman, E.A., 2001. Propagation of intercellular calcium waves in retinal astrocytes and Muller cells. The Journal of neuroscience : the official journal of the Society for Neuroscience 21, 2215-2223.

Nicchia, G.P., Frigeri, A., Liuzzi, G.M., Santacroce, M.P., Nico, B., Procino, G., Quondamatteo, F., Herken, R., Roncali, L., Svelto, M., 2000. Aquaporin-4-containing astrocytes sustain a temperature- and mercury-insensitive swelling in vitro. Glia 31, 29-38.

Nicchia, G.P., Frigeri, A., Liuzzi, G.M., Svelto, M., 2003. Inhibition of aquaporin-4 expression in astrocytes by RNAi determines alteration in cell morphology, growth, and water transport and induces changes in ischemia-related genes. FASEB journal : official publication of the Federation of American Societies for Experimental Biology 17, 1508-1510.

Nicchia, G.P., Rossi, A., Nudel, U., Svelto, M., Frigeri, A., 2008. Dystrophin-dependent and -independent AQP4 pools are expressed in the mouse brain. Glia 56, 869-876.

Nicchia, G.P., Srinivas, M., Li, W., Brosnan, C.F., Frigeri, A., Spray, D.C., 2005. New possible roles for aquaporin-4 in astrocytes: cell cytoskeleton and functional relationship with connexin43. Faseb J 19, 1674-1676.

Owler, B.K., Pitham, T., Wang, D., 2010. Aquaporins: relevance to cerebrospinal fluid physiology and therapeutic potential in hydrocephalus. Cerebrospinal Fluid Res 7:15.

Pannicke, T., Wurm, A., Iandiev, I., Hollborn, M., Linnertz, R., Binder, D.K., Kohen, L., Wiedemann, P., Steinhauser, C., Reichenbach, A., Bringmann, A., 2010. Deletion of aquaporin-4 renders retinal glial cells more susceptible to osmotic stress. J Neurosci Res 88, 2877-2888.

Pisani, F., Mola, M.G., Simone, L., Rosito, S., Alberga, D., Mangiatordi, G.F., Lattanzi, G., Nicolotti, O., Frigeri, A., Svelto, M., Nicchia, G.P., 2014. Identification of a point mutation impairing the binding between aquaporin-4 and neuromyelitis optica autoantibodies. J Biol Chem 289, 30578-30589.

Qin, Y., Ren, H., Hoffman, M.R., Fan, J., Zhang, M., Xu, G., 2012. Aquaporin changes during diabetic retinopathy in rats are accelerated by systemic hypertension and are linked to the renin-angiotensin system. Invest Ophthalmol Vis Sci 53, 3047-3053.

Shelton, M.D., Distler, A.M., Kern, T.S., Mieyal, J.J., 2009. Glutaredoxin regulates autocrine and paracrine proinflammatory responses in retinal glial (muller) cells. The Journal of biological chemistry 284, 4760-4766.

Stone, J., Dreher, Z., 1987. Relationship between astrocytes, ganglion cells and vasculature of the retina. The Journal of comparative neurology 255, 35-49.

Verderber, L., Johnson, W., Mucke, L., Sarthy, V., 1995. Differential regulation of a glial fibrillary acidic protein-LacZ transgene in retinal astrocytes and Muller cells. Investigative ophthalmology & visual science 36, 1137-1143.

Verkhratsky, A., Anderova, M., Chvatal, A., 2009. Differential calcium signalling in neuronal-glial networks. Front Biosci (Landmark Ed) 14, 2004-2016.

Verkhratsky, A., Sofroniew, M.V., Messing, A., deLanerolle, N.C., Rempe, D., Rodriguez, J.J., Nedergaard, M., 2012. Neurological diseases as primary gliopathies: a reassessment of neurocentrism. ASN Neuro 4.

Verkman, A.S., Ruiz-Ederra, J., Levin, M.H., 2008. Functions of aquaporins in the eye. Prog Retin Eye Res 27, 420-433.

Wang, J., Xu, X., Elliott, M.H., Zhu, M., Le, Y.Z., 2010. Muller cell-derived VEGF is essential for diabetes-induced retinal inflammation and vascular leakage. Diabetes 59, 2297-2305.

Yang, B., Verkman, A.S., 1997. Water and glycerol permeabilities of aquaporins 1-5 and MIP determined quantitatively by expression of epitope-tagged constructs in Xenopus oocytes. J Biol Chem 272, 16140-16146.

Figure legends

Figure 1: Analysis of intraretinal vasculature by isolectin staining in WT and AQP4 KO mice. A) Drawing of mouse retina highlighting the relationship between the intraretinal vasculature and glial cells. In red are shown the superficial (primary), the intermediate (inner deeper) and deep (outer deeper) plexi. The superficial plexus in mouse retina is localised at the NFL/GCL interface while the intermediate and deep plexi are at the IPL and OPL, respectively. Note that the superficial plexus is mainly ensheathed by astrocytes (green cells) while the intermediate and deep plexi are ensheathed by Müller cells (blue cells). (NFL, Nerve Fibre Layer; GCL, Ganglion Cell Layer; IPL, Inner Plexiform Layer; INL, Inner Nuclear Layer; OPL, Outer Plexiform Layer; ONL, Outer Nuclear Layer). B) xy confocal microscopy images of superficial, intermediate and deep plexi stained with anti-GFAP (blue) and anti-AQP4 (red) antibodies and IB4 (green). Scale bar 50 µm. C) z-stack (24 µm) image showing GFAP, AQP4 and IB4 signal distribution within the thickness of the retina. The colour is representative of the depth of the immunofluorescence signal, from red (top) to blue (bottom). D) xy confocal microscopy analysis of superficial, intermediate and deep plexi of WT and AQP4 KO retinas stained with IB4. Scale bar 100 µm.

Figure 2: Analysis of AQP4 depending BRB functionality by Evans blue assay. A) Left, epifluorescence images of Evans blue injected WT and AQP4 KO retinas. Extravasations are highlighted by arrowheads. Right, histogram showing the number of extravasations measured in WT and AQP4 KO mice. Scale bar 50 µm (*P<0.001, n=12). Representative xz (B) and xy (C) confocal microscopy acquisitions from the experiments described in (A) for AQP4 KO retinas. Note that the main site of extravasations (white arrow) is the deep plexus. Scale bar 30 µm.

Figure 3: Immunofluorescence and Western blot analysis of Glutamine Synthetase expression in AQP4 KO retina. A) Representative epifluorescence images of Glutamine Synthetase (GS) expression (green) in retinal sections prepared from WT and AQP4 KO mice. Nuclei (DAPI, blue), AQP4 (red) and merge are shown. GS immunoreactivity in the AQP4 KO shows no evident changes in expression and distribution compared to WT. Scale bar 50 µm. B,C) Western blot (B) and histogram (C) showing GS expression and densitometry analysis in WT and AQP4 KO mouse retina. GAPDH was used as an internal control for protein loading (n=8).

Figure 4: Immunofluorescence, Western blot and qPCR analysis of GFAP expression in AQP4 KO retina. A) Representative epifluorescence images of GFAP expression (green) in retinal sections prepared from WT and AQP4 KO mice. Nuclei (DAPI, blue), AQP4 (red) and merge are shown. Scale bar 50 µm. B) Draw of the three GFAP isoforms (α, δ, and k) analysed by Western blot (C, D) and qPCR (E). The red asterisk in exon-7 shows the epitope for the anti-GFAP G-A-5 monoclonal antibody used. C) Western blot showing GFAPα, δ and k isoform expression in WT and AQP4 KO mouse retina. Actin was used as an internal control for protein loading. D) Histograms summarizing the actin normalized densitometry analysis of single GFAP isoforms (α, δ, and k) or total GFAP (TOT) E) Histograms showing GFAPα, δ, and k mRNA levels detected by qPCR. Results are reported as GAPDH-normalized AQP4 KO /WT (*P<0.05, **P<0.005, ***P<0.0005; n=8 and n=3 for experiments shown in panels D and E, respectively).

Figure 5: Analysis of GFAP expression in WT and AQP4 KO whole mount retina. Confocal microscopy analysis of GFAP (yellow) immunolocalization in WT and AQP4 KO mouse whole retina; in red the endothelial marker CD31. GFAP is over-expressed in AQP4 KO

superficial plexus while no alterations were found at the level of the intermediate or deep plexus. Scale bar 50 µm.

Figure 6: Analysis of AQP4 and GFAP expression in AQP4 siRNA treated primary astrocyte cultures. Western blot showing AQP4 and GFAP expression in rat and mouse astrocytes treated with CTRL and AQP4 siRNA. No GFAP alteration was observed after ten days of AQP4 siRNA treatment either in rat or in mouse astrocytes. GAPDH was used as an internal control for protein loading (n=8).

Figure 7: mRNA increased expression of inflammatory markers in the retina of AQP4 KO mice**.** Scatter plot showing Tumor Necrosis Factor-α (TNF-α), Intercellular Adhesion Molecule1 (ICAM-1), Interleukin-1β (IL-1β) and Interleukin-6 (IL-6) mRNA levels in retinas of WT and AQP4 KO mice (*P<0.05, **P<0.005, ***P<0.0005; n=7).

Figure 1

Click here to download high resolution image

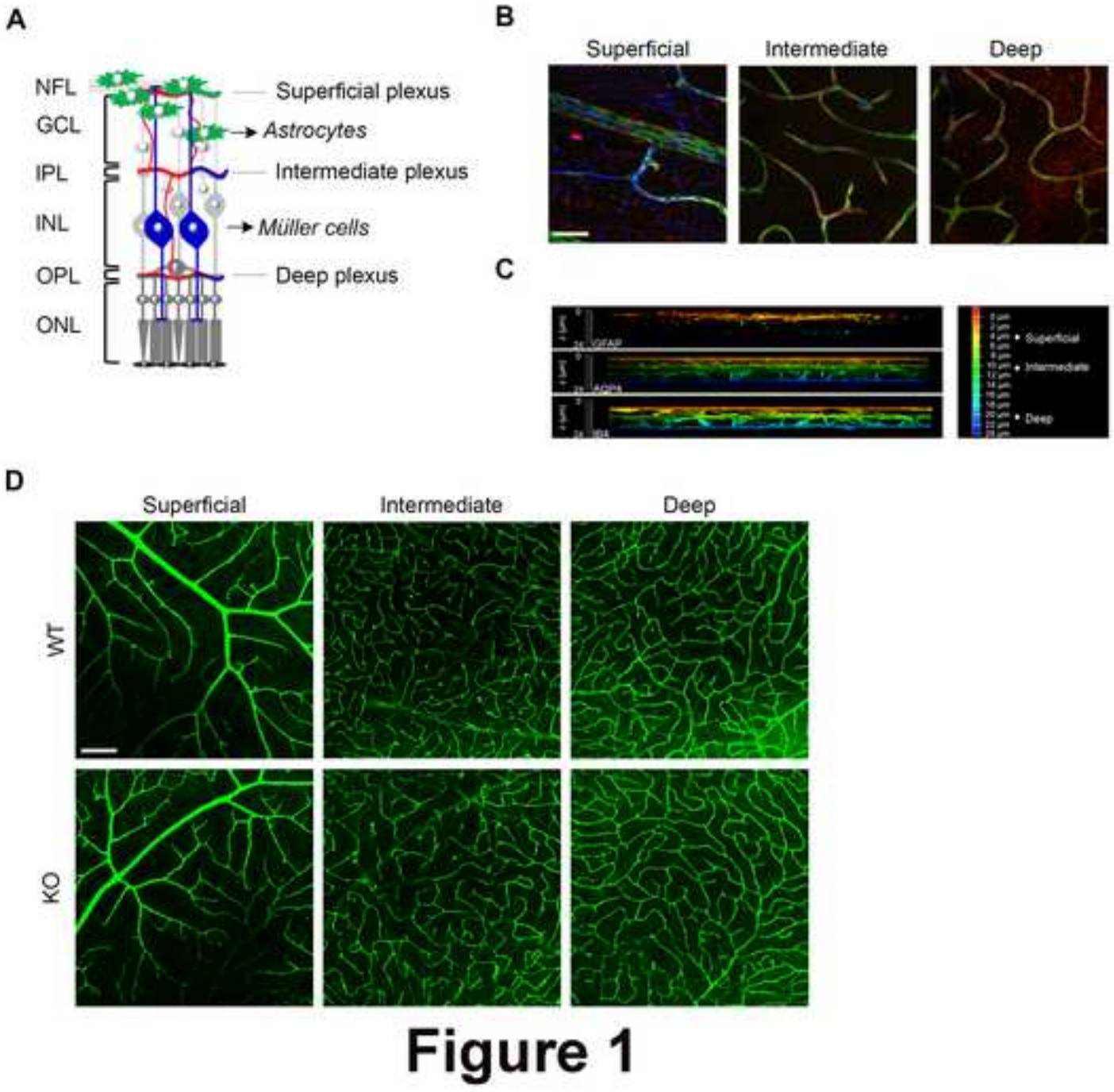

Figure 1

Figure 2
Click here to download high resolution image

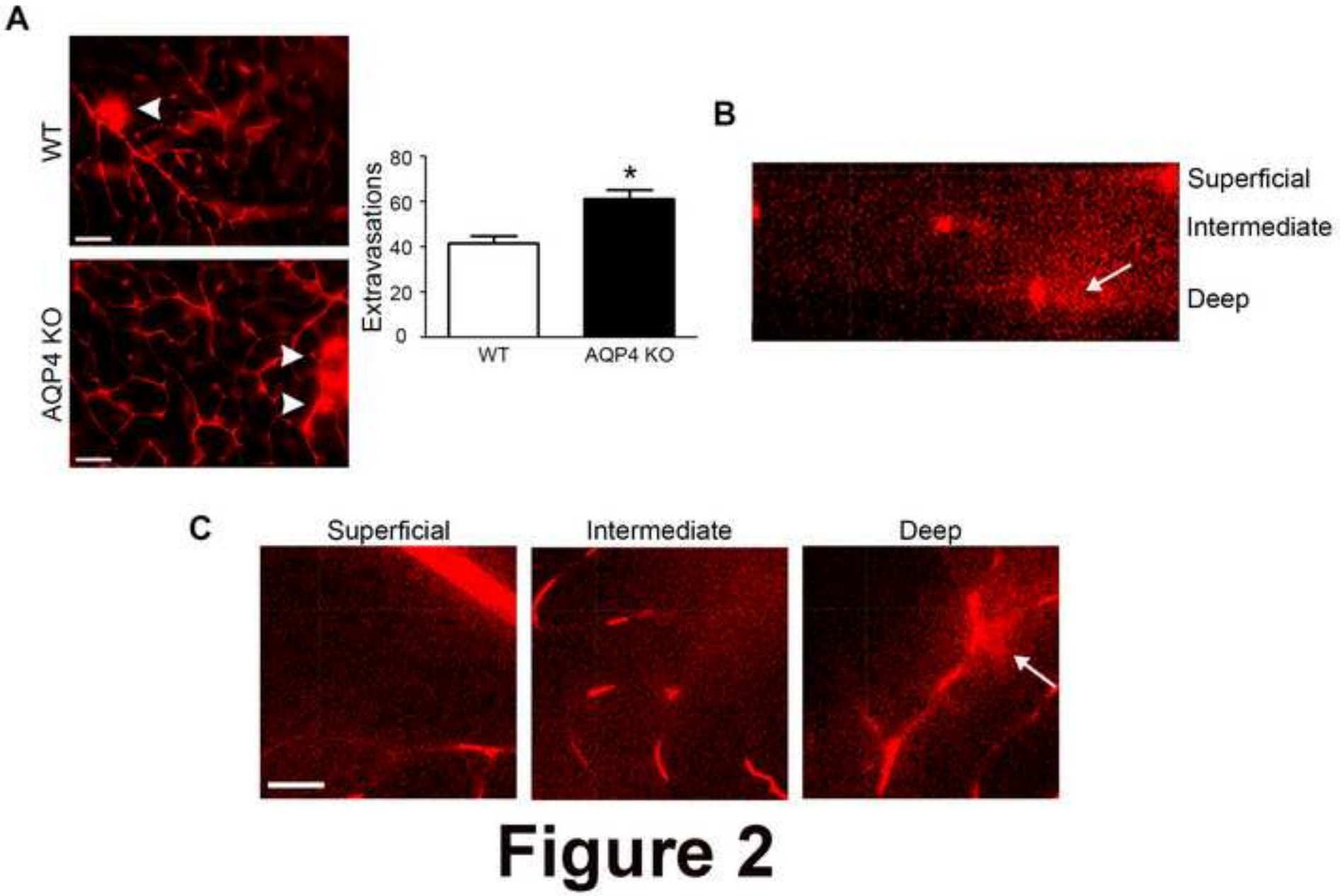

Figure 2

Figure 3

Click here to download high resolution image

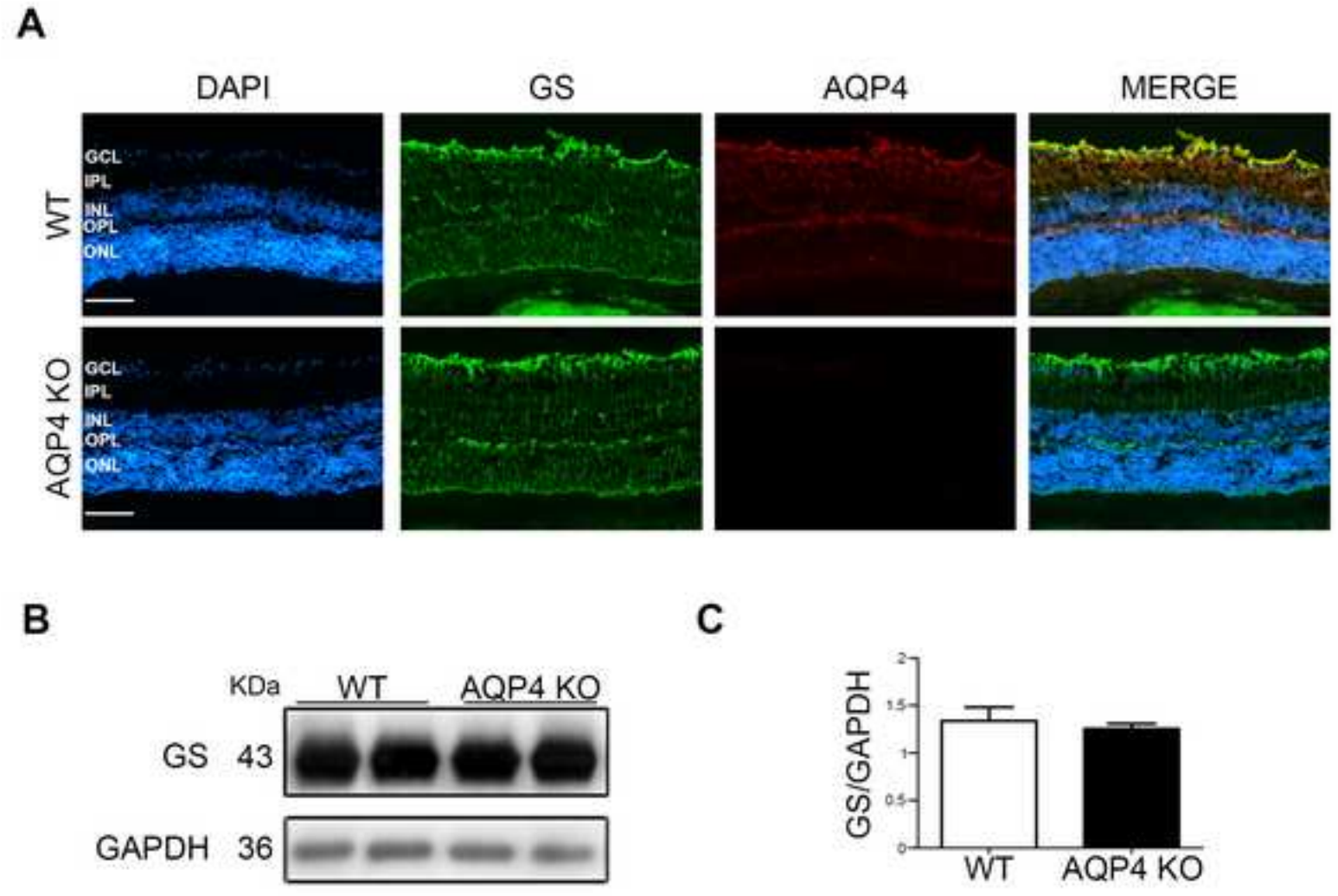

Figure 3

Figure 4
Click here to download high resolution image

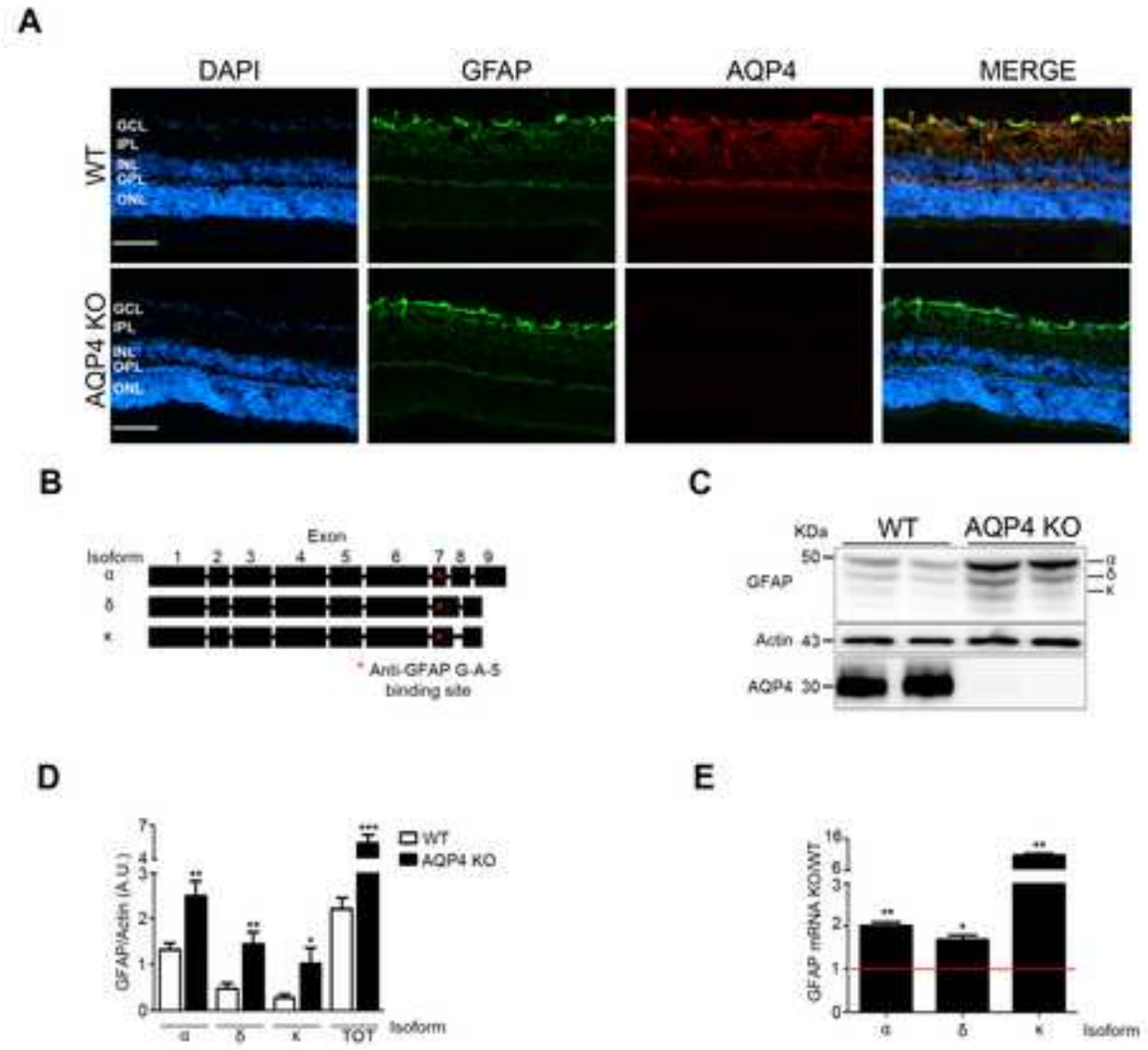

Figure 4

Figure 5

Click here to download high resolution image

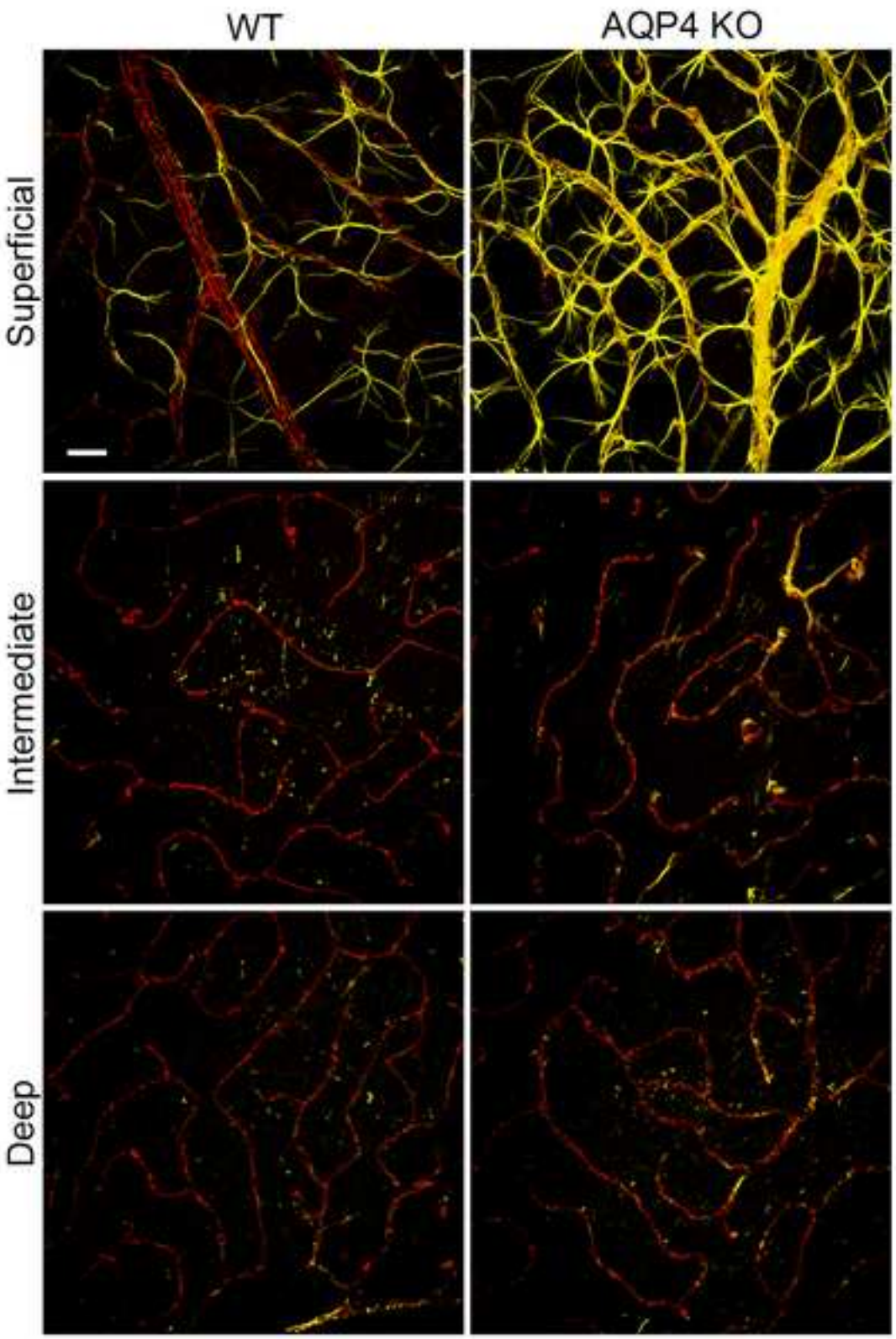

Figure 5

Figure 6

Click here to download high resolution image

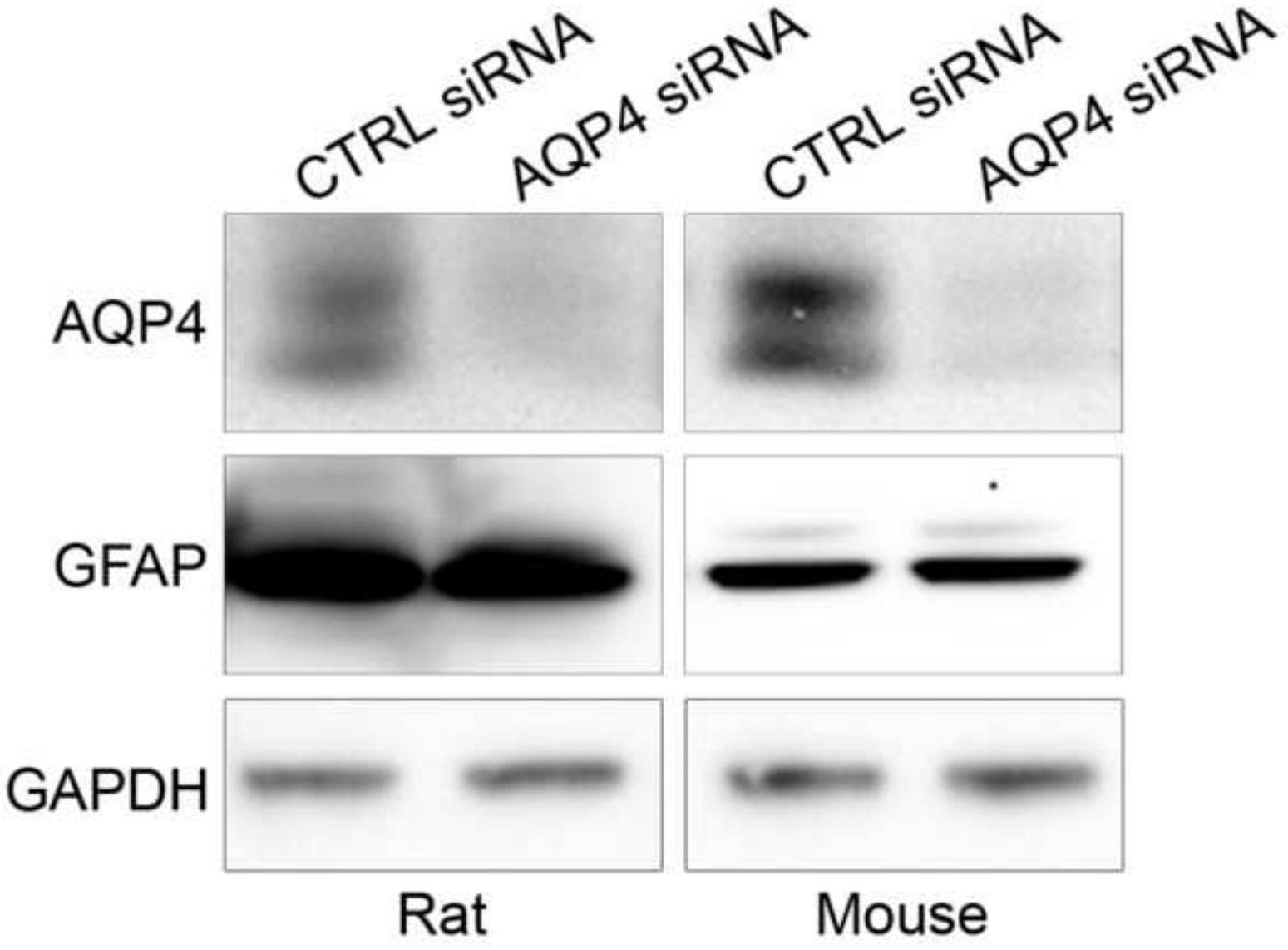

Figure 6

Figure 7

Click here to download high resolution image

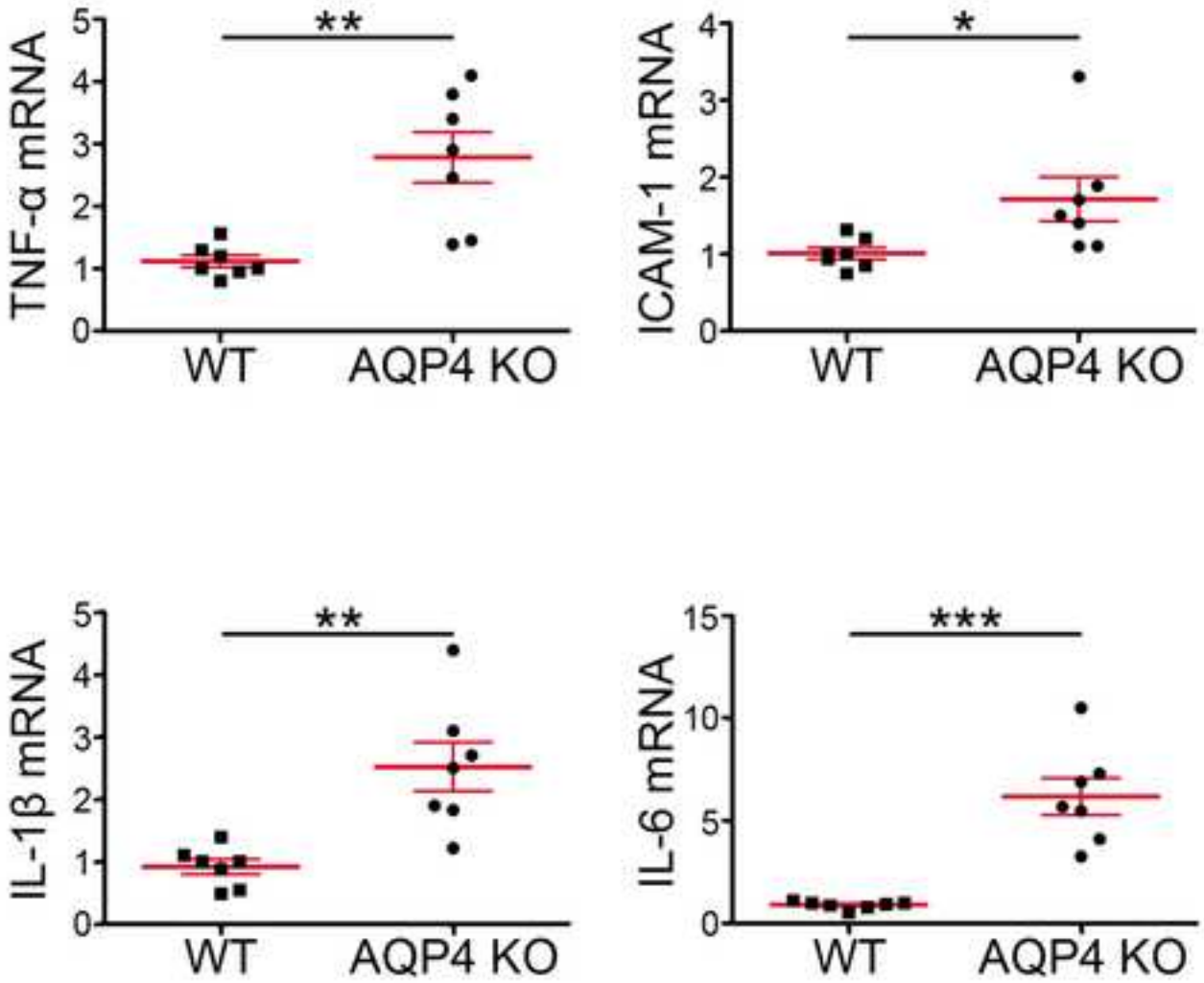

Figure 7